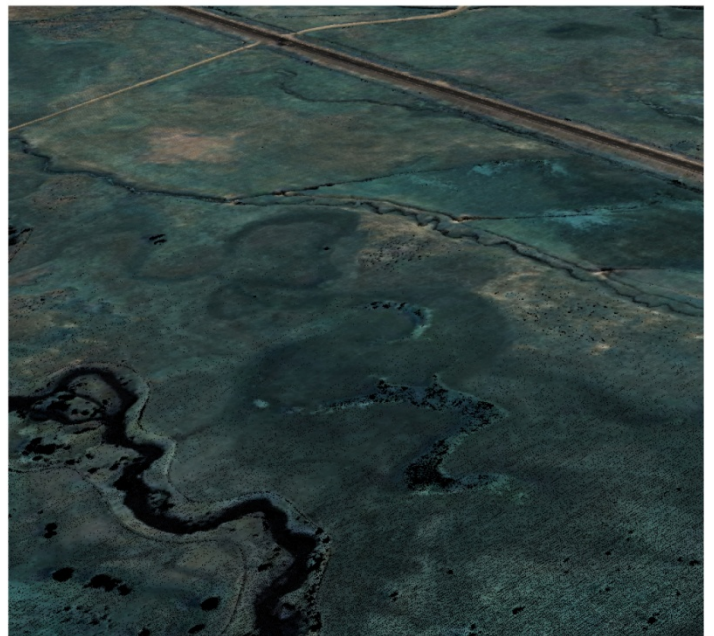


LiDAR REMOTE SENSING

LEMHI RIVER • IDAHO

(1/11/2011)



TROUT UNLIMITED • KIM TROTTER - 151 N. Ridge Ave., Suite 120 - Idaho Falls, ID 83402

UTAH STATE UNIVERSITY • JOE WHEATON - 5210 Old Main Hill - Logan UT 84322

 **WATERSHED SCIENCES** • 517 SW 2nd Street, Suite 400 - Corvallis, OR 97333

LIDAR REMOTE SENSING DATA COLLECTION AND TRUE-COLOR ORTHOPHOTOGRAPHS: LEMHI RIVER, ID

TABLE OF CONTENTS

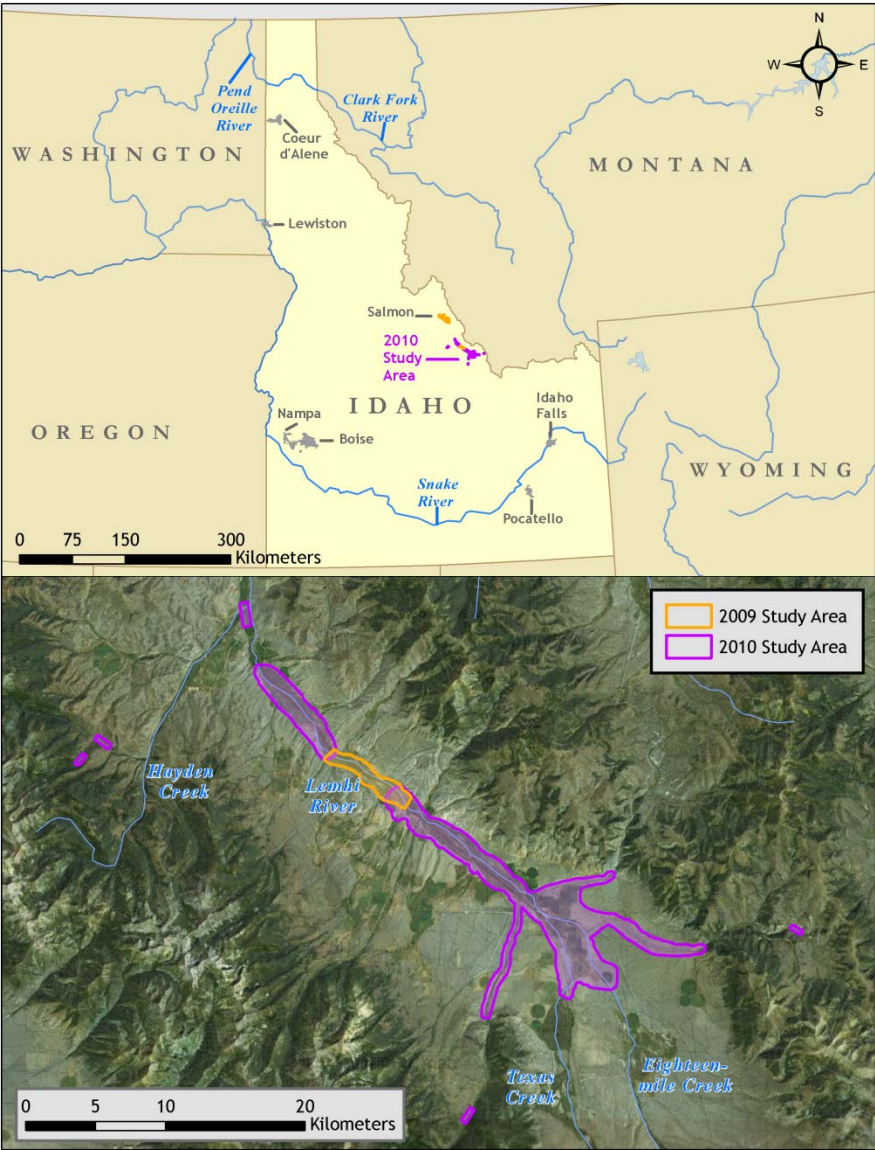
1. Overview	1
2. Acquisition	2
2.1 Airborne Survey - Instrumentation and Methods	2
2.2 Ground Survey - Instrumentation and Methods	3
2.2.1 Instrumentation	3
2.2.2 Monumentation	3
2.2.3 Methodology	4
3. LiDAR Data Processing	7
3.1 Applications and Work Flow Overview	7
3.2 Aircraft Kinematic GPS and IMU Data	8
3.3 Laser Point Processing	8
3.3.1 Vegetation Classification	10
3.4 Orthophotograph Processing	10
4. LiDAR Accuracy Assessment	11
4.1 Laser Noise and Relative Accuracy	11
4.2 Absolute Accuracy	12
5. Photo Accuracy Assessment	13
6. Study Area Results	14
6.1 Data Summary	14
6.2 Data Density/Resolution	14
6.3 Relative Accuracy Calibration Results	18
6.4 Absolute Accuracy	19
6.5 Orthophotograph Accuracy	20
7. Model Development	22
7.1 Breakline Enforced Terrain Model	22
7.2 Vegetation Surface Model	24
8. Contours	25
9. Projection/Datum and Units	26
10. Deliverables	26
11. Selected Images	27
12. Glossary	35
13. Citations	36
Appendix A	37



1. Overview

From September 24 - 26, 2010, Watershed Sciences, Inc. (WSI) collected Light Detection and Ranging (LiDAR) data and true-color orthophotographs for two mainstem areas of interest (AOI) along the Lemhi River for Trout Unlimited (partnering with the Bureau of Reclamation) and at five additional 'satellite' AOIs added to the acquisition by Utah State University. This report documents the data acquisition, processing methods, accuracy assessment, and deliverables for the 2010 remote sensing data collection. The requested area was expanded to include a 100m buffer to ensure complete coverage and adequate point densities around survey area boundaries. The 2010 Lemhi River data were integrated with overlapping portions of the 2009 data (Amonson) to provide seamless models. The total acreage of this delivery is 19,673 acres of LiDAR and orthophotos (Figure 1, purple).

Figure 1. Lemhi River areas of interest in NE Idaho.



2. Acquisition

2.1 Airborne Survey - Instrumentation and Methods

The LiDAR survey utilized dual-mounted Leica ALS50 Phase II sensors in a Cessna Caravan 208B. The ALS50 Phase II sensor operates with Automatic Gain Control (AGC) for intensity correction. The Leica systems were set to acquire $\geq 83,000$ laser pulses per second (i.e., 83 kHz pulse rate) and flown at 1300 meters above ground level (AGL), capturing a scan angle of $\pm 14^\circ$ from nadir. These settings are developed to yield points with an average native pulse density of ≥ 8 pulses per square meter over terrestrial surfaces. It is not uncommon for some types of surfaces (e.g. dense vegetation or water) to return fewer pulses than the laser originally emitted. These discrepancies between ‘native’ and ‘delivered’ density will vary depending on terrain, land cover, and the prevalence of water bodies.



The Cessna Caravan is a stable platform, ideal for flying slow and low for high density projects. The Leica ALS50 sensor head installed in the Caravan is shown on the left.

All areas were surveyed with an opposing flight line side-lap of $\geq 50\%$ ($\geq 100\%$ overlap) to reduce laser shadowing and increase surface laser painting. The Leica laser systems allow up to four range measurements (returns) per pulse, and all discernable laser returns were processed for the output dataset.

To accurately solve for laser point position (geographic coordinates x, y, z), the positional coordinates of the airborne sensor and the attitude of the aircraft were recorded continuously throughout the LiDAR data collection mission. Aircraft position was measured twice per second (2 Hz) by an onboard differential GPS unit. Aircraft attitude was measured 200 times per second (200 Hz) as pitch, roll and yaw (heading) from an onboard inertial measurement unit (IMU). To allow for post-processing correction and calibration, aircraft/sensor position and attitude data are indexed by GPS time.

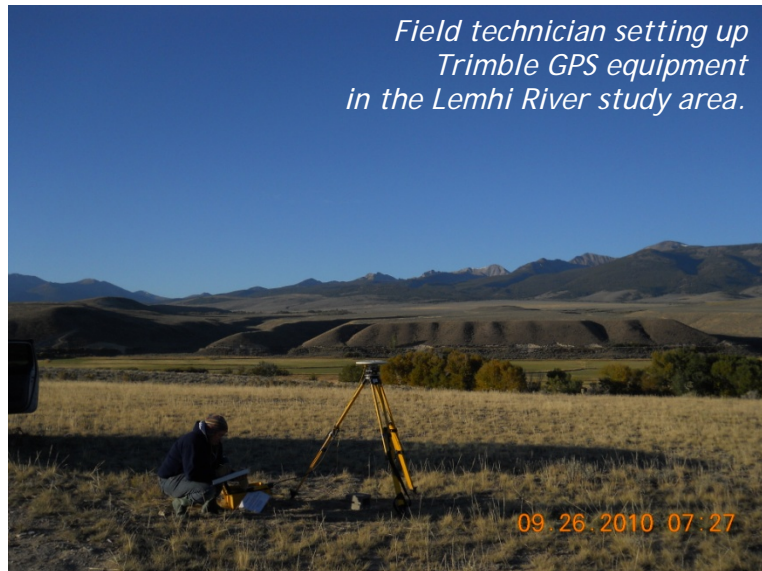
The aerial imagery was collected using a Leica RCD-105 39 megapixel digital camera. For the Lemhi River study area, the images were collected in 3 spectral bands (red, green, blue) with 60% along track overlap and 30% sidelap between frames. The acquisition flight parameters were designed to yield native pixel resolution of ≤ 14 cm.

LiDAR Data Acquisition and Processing: Lemhi River, ID

Prepared by Watershed Sciences, Inc.

2.2 Ground Survey - Instrumentation and Methods

During the LiDAR survey, static (1 Hz recording frequency) ground surveys were conducted over set monuments. Monument coordinates are provided in Table 1 and shown in Figure 2 for the AOI. After the airborne survey, the static GPS data are processed using triangulation with Continuously Operating Reference Stations (CORS) and checked using the Online Positioning User Service (OPUS¹) to quantify daily variance. Multiple sessions are processed over the same monument to confirm antenna height measurements and reported position accuracy.



Indexed by time, these GPS data are used to correct the continuous onboard measurements of aircraft position recorded throughout the mission. Control monuments were located within 13 nautical miles of the survey area.

2.2.1 Instrumentation

For this delivery area, a Trimble GPS receiver model R7 with Zephyr Geodetic antenna with ground plane was deployed for all static control. A Trimble model R8 GNSS unit was used for collecting check points using real time kinematic (RTK) survey techniques. For RTK data, the collector begins recording after remaining stationary for 5 seconds then calculating the pseudo range position from at least three epochs with the relative error under 1.5 cm horizontal and 2 cm vertical. All GPS measurements are made with dual frequency L1-L2 receivers with carrier-phase correction.



2.2.2 Monumentation

The Watershed Sciences' monumentation was implemented with 5/8" x 30" rebar topped with a metal cap stamped with the project ID and year.

Watershed Sciences incorporated two control monuments provided by Matthew J McKeegan, P.L.S. of McKeegan Associates, Inc. (S4_01 & S7_01). Monuments selected were found to have good visibility and optimal location to support a LiDAR Acquisition flight.

Table 1. Base Station control coordinates for Lemhi River.

¹ Online Positioning User Service (OPUS) is run by the National Geodetic Survey to process corrected monument positions.

Base Station ID	Datum: NAD83 (CORS96)		GRS80
	Latitude	Longitude	Ellipsoid Z (meters)
LEM_02	44° 41' 17.52894	113° 20' 28.09751	1824.244
LEM_03	44° 46' 52.78174	113° 32' 20.99481	1681.754
S4_01	44° 45' 15.84500	113° 29' 7.93377	1701.139
S7_01	44° 39' 47.24385	113° 22' 34.19852	1843.341

2.2.3 Methodology



Each aircraft is assigned a ground crew member with two Trimble R7 receivers and an R8 receiver. The ground crew vehicles are equipped with standard field survey supplies and equipment including safety materials. All control monuments are observed for a minimum of two survey sessions lasting no fewer than 6 hours. At the beginning of every session the tripod and antenna are reset, resulting in two independent instrument heights and data files. Data is collected at a rate of 1Hz using a 10 degree mask on the antenna.

The ground crew uploads the GPS data to our FTP site on a daily basis to be returned to the office for Professional Land Surveyor (PLS) oversight, QA/QC review and processing. OPUS processing triangulates the monument position using 3 CORS stations resulting in a fully adjusted position. After multiple days of data have been collected at each monument, accuracy and error ellipses are calculated from the OPUS reports. This information leads to a rating of the monument based on FGDC-STD-007.2-1998² Part 2 table 2.1 at the 95% confidence level. When a statistical stable position is found CORPSCON³ 6.0.1 software is used to convert the UTM positions to geodetic positions. This geodetic position is used for processing the LiDAR data.

RTK and aircraft mounted GPS measurements are made during periods with PDOP⁴ less than or equal to 3.0 and with at least 6 satellites in view of both a stationary reference receiver and the roving receiver. Static GPS data collected in a continuous session average the high PDOP into the final solution in the method used by CORS stations. RTK positions are collected on bare earth locations such as paved, gravel or stable dirt roads, and other locations where the

² Federal Geographic Data Committee Draft Geospatial Positioning Accuracy Standards

³ U.S. Army Corps of Engineers, Engineer Research and Development Center Topographic Engineering Center software

⁴PDOP: Point Dilution of Precision is a measure of satellite geometry, the smaller the number the better the geometry between the point and the satellites.

LiDAR Data Acquisition and Processing: Lemhi River, ID

ground is clearly visible (and is likely to remain visible) from the sky during the data acquisition and RTK measurement period(s).

In order to facilitate comparisons with LiDAR measurements, RTK measurements are not taken on highly reflective surfaces such as center line stripes or lane markings on roads. RTK points were taken no closer than one meter to any nearby terrain breaks such as road edges or drop offs.

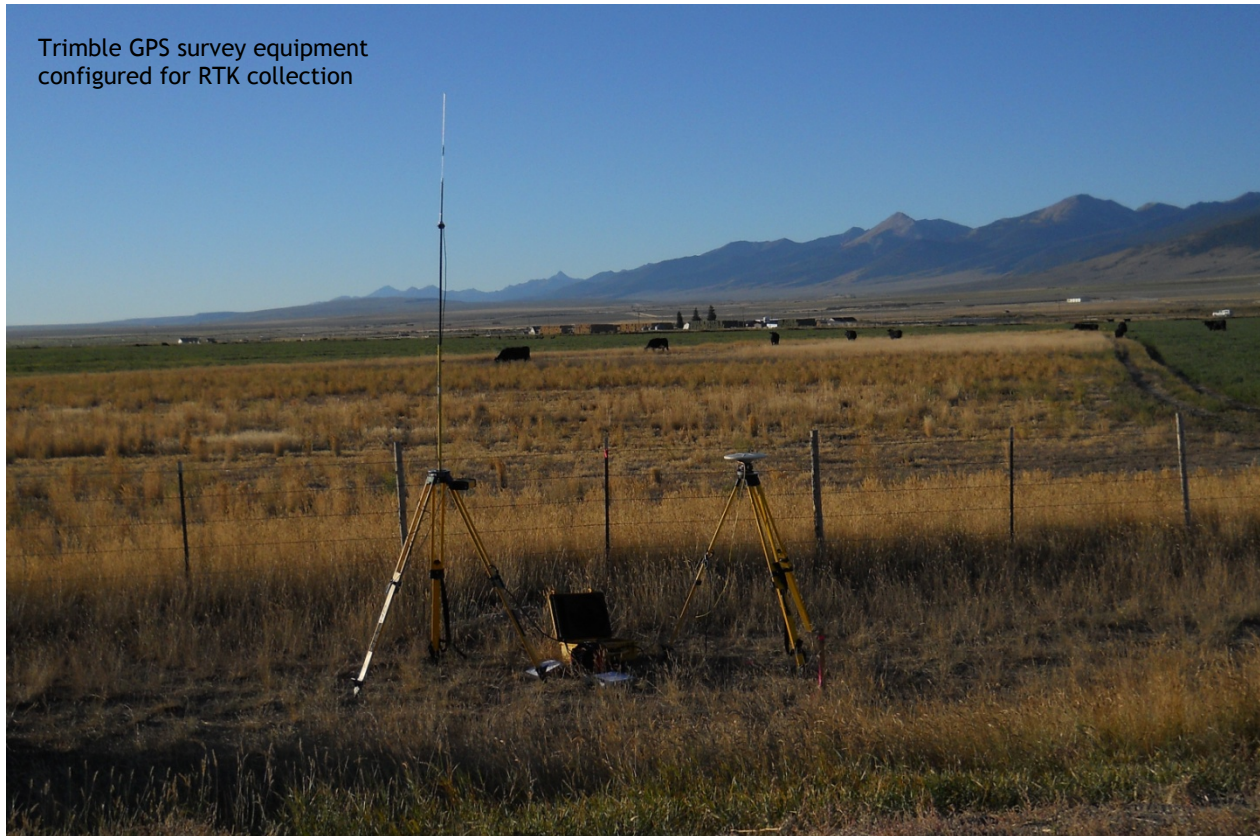
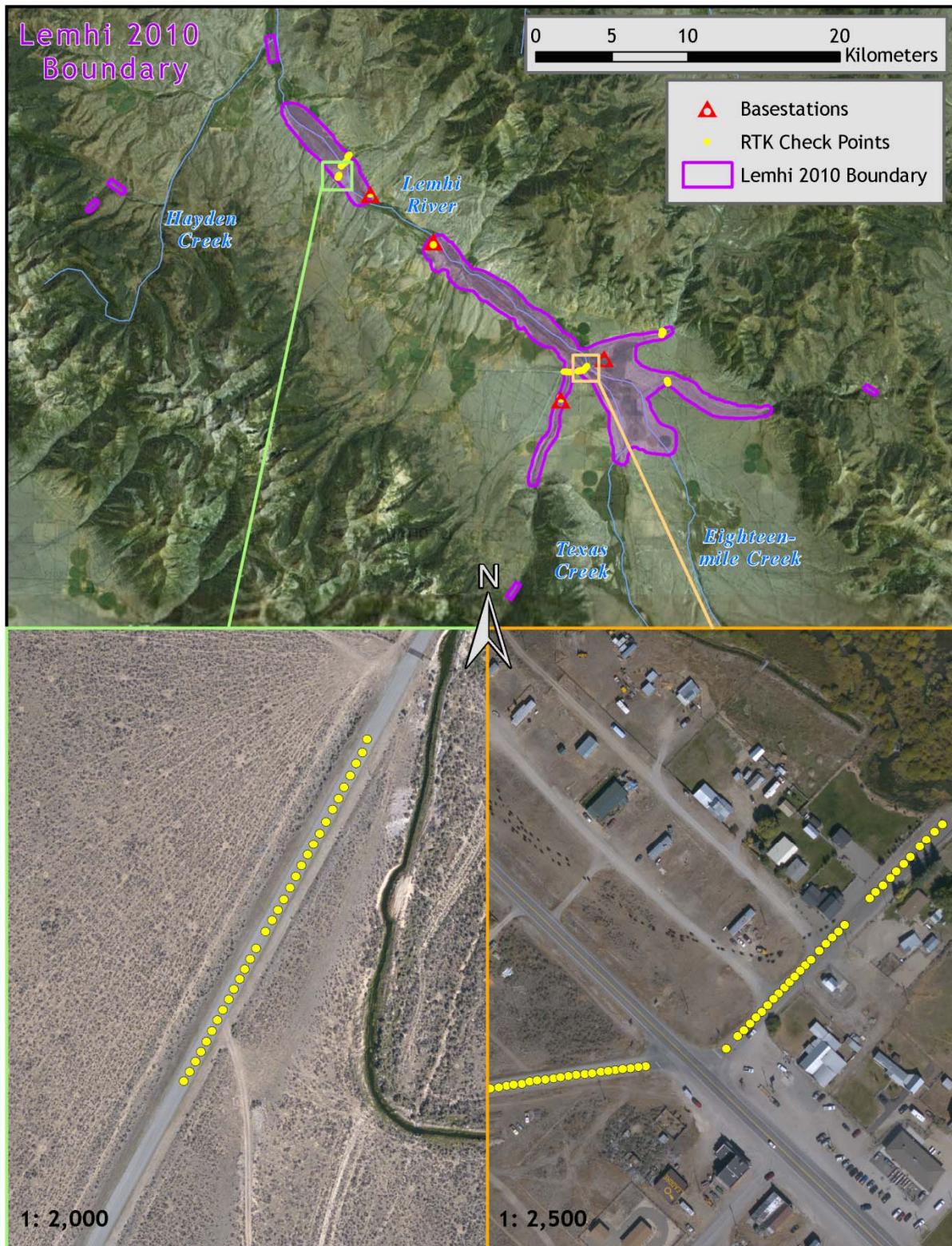


Figure 2. RTK check point and control monument locations used in the Lemhi River AOIs.



3. LiDAR Data Processing

3.1 Applications and Work Flow Overview

1. Resolved kinematic corrections for aircraft position data using kinematic aircraft GPS and static ground GPS data.
Software: Waypoint GPS v.8.10, Trimble Geomatics Office v.1.62
2. Developed a smoothed best estimate of trajectory (SBET) file that blends post-processed aircraft position with attitude data. Sensor head position and attitude were calculated throughout the survey. The SBET data were used extensively for laser point processing.
Software: IPAS v.1.35
3. Calculated laser point position by associating SBET position to each laser point return time, scan angle, intensity, etc. Created raw laser point cloud data for the entire survey in *.las (ASPRS v. 1.2) format.
Software: ALS Post Processing Software v.2.70
4. Imported raw laser points into manageable blocks (less than 500 MB) to perform manual relative accuracy calibration and filter for pits/birds. Ground points were then classified for individual flight lines (to be used for relative accuracy testing and calibration).
Software: TerraScan v.10.009
5. Using ground classified points per each flight line, the relative accuracy was tested. Automated line-to-line calibrations were then performed for system attitude parameters (pitch, roll, heading), mirror flex (scale) and GPS/IMU drift. Calibrations were performed on ground classified points from paired flight lines. Every flight line was used for relative accuracy calibration.
Software: TerraMatch v.10.006
6. Position and attitude data were imported. Resulting data were classified as ground and non-ground points. Statistical absolute accuracy was assessed via direct comparisons of ground classified points to ground RTK survey data. Data were then converted to orthometric elevations (NAVD88) by applying a Geoid03 correction.
Software: TerraScan v.10.009, TerraModeler v.10.004
7. Bare Earth models were created as a triangulated surface and exported as ArcInfo ASCII grids at a 1-meter pixel resolution. Highest Hit models were created for any class at 1-meter grid spacing and exported as ArcInfo ASCII grids.
Software: TerraScan v.10.009, ArcMap v. 9.3.1, TerraModeler v.10.004
8. Converted raw images to tif format, calibrating raw image pixels for gain and exposure settings of each image.
Software: Leica Calibration Post Processing v.1.0.4
9. Calculated photo position and orientation by associating the SBET position (Step 3) to each image capture time.
Software: IPASCO v.1.3
10. Orthorectified calibrated tiffs utilizing photo orientation information (Step 8) and the LiDAR-derived ground surface (Step 6).

Software: Leica Photogrammetry Suite (LPS) v.9.2

11. To correct light imbalances between overlapping images, radiometric global tilting adjustments were applied to the rectified images.

Software: OrthoVista v.4.4.

12. The color corrected images were then mosaicked together for the survey area and subset into tiles to make the file size more manageable.

Software: OrthoVista v.4.4.

13. Mosaicked tiles were inspected for misalignments introduced by automatic seam generation. Misalignments were corrected by manual adjustments to seams.

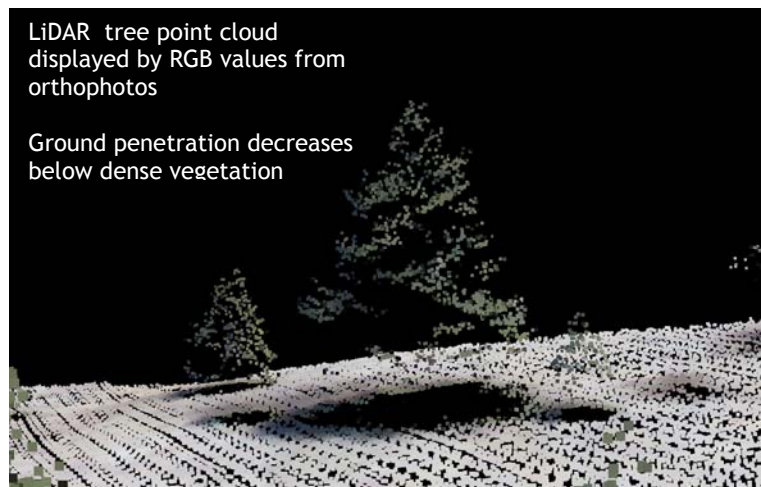
Software: Adobe Photoshop 7.0, OrthoVista v.4.4.

3.2 Aircraft Kinematic GPS and IMU Data

LiDAR survey datasets were referenced to the 1 Hz static ground GPS data collected over pre-surveyed monuments with known coordinates. While surveying, the aircraft collected 2 Hz kinematic GPS data, and the onboard inertial measurement unit (IMU) collected 200 Hz aircraft attitude data. Waypoint GPS v.8.10 was used to process the kinematic corrections for the aircraft. The static and kinematic GPS data were then post-processed after the survey to obtain an accurate GPS solution and aircraft positions. IPAS v.1.35 was used to develop a trajectory file that includes corrected aircraft position and attitude information. The trajectory data for the entire flight survey session were incorporated into a final smoothed best estimated trajectory (SBET) file that contains accurate and continuous aircraft positions and attitudes.

3.3 Laser Point Processing

Laser point coordinates were computed using the IPAS and ALS Post Processor software suites based on independent data from the LiDAR system (pulse time, scan angle), and aircraft trajectory data (SBET). Laser point returns (first through fourth) were assigned an associated (x, y, z) coordinate along with unique intensity values (0-255). The data were output into large LAS v. 1.2 files with each point maintaining the corresponding scan angle, return number (echo), intensity, and x, y, z (easting, northing, and elevation) information.



These initial laser point files were too large for subsequent processing. To facilitate laser point processing, bins (polygons) were created to divide the dataset into manageable sizes (< 500 MB). Flightlines and LiDAR data were then reviewed to ensure complete coverage of the survey area and positional accuracy of the laser points.

Laser point data were imported into processing bins in TerraScan, and manual calibration was performed to assess the system offsets for pitch, roll, heading and scale (mirror flex). Using a geometric relationship developed by Watershed Sciences, each of these offsets was resolved and corrected if necessary.

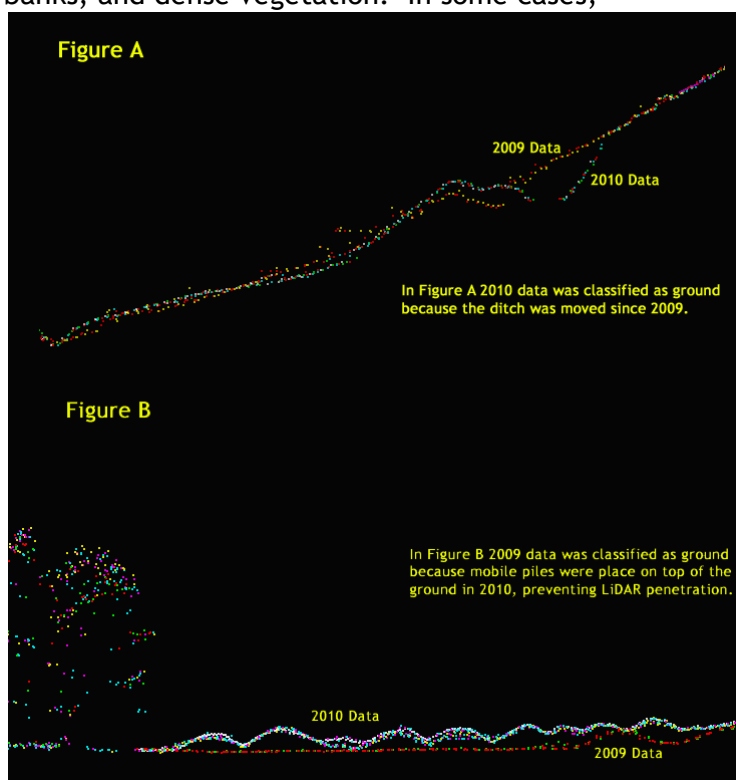
LiDAR points were then filtered for noise, pits (artificial low points), and birds (true birds as well as erroneously high points) by screening for absolute elevation limits, isolated points and height above ground. Each bin was then manually inspected for remaining pits and birds and spurious points were removed. In a bin containing approximately 7.5-9.0 million points, an average of 50-100 points are typically found to be artificially low or high. Common sources of non-terrestrial returns are clouds, birds, vapor, haze, decks, brush piles, etc.

Internal calibration was refined using TerraMatch. Points from overlapping lines were tested for internal consistency and final adjustments were made for system misalignments (i.e., pitch, roll, heading offsets and scale). Automated sensor attitude and scale corrections yielded 3-5 cm improvements in the relative accuracy. Once system misalignments were corrected, vertical GPS drift was then resolved and removed per flight line, yielding a slight improvement (<1 cm) in relative accuracy.

The TerraScan software suite is designed specifically for classifying near-ground points (Soininen, 2004). The processing sequence began by ‘removing’ all points that were not ‘near’ the earth based on geometric constraints used to evaluate multi-return points. The resulting bare earth (ground) model was visually inspected and additional ground point modeling was performed in site-specific areas to improve ground detail. This manual editing of ground often occurs in areas with known ground modeling deficiencies, such as: bedrock outcrops, cliffs, deeply incised stream banks, and dense vegetation. In some cases, automated ground point classification erroneously included known vegetation (i.e., understory, low/dense shrubs, etc.). These points were manually reclassified as default. Ground surface rasters were then developed from triangulated irregular networks (TINs) of ground points.

For the 2009/2010 data integration, we observed some divergence among ground surfaces within a few select areas (Figure 2). These were evaluated and resolved individually to preserve an accurate bare earth model across the study area.

Figure 3. Examples of issues encountered when integrating 2009 and 2010 LiDAR data.



3.3.1 Vegetation Classification

Classification of vegetation points was a two-part process. First, man-made structures and mobile devices were manually removed from the default class in the LiDAR point cloud. Second, to exclude any spurious points due to laser noise from the vegetation model, the remaining LiDAR points were reclassified as vegetation, using an automated process with a 25 centimeter height-from-ground threshold. Because the Lemhi River study area has a high occurrence of agricultural fields where agricultural practices may have introduced changes in land cover during the time span of the LiDAR flight, the vegetation model may contain discrepancies in height values within the same x,y locations. These discrepancies were unavoidable and should be considered in any application of this model. Figure 4 illustrates an example of such discrepancies observed in the Lemhi River vegetation model.

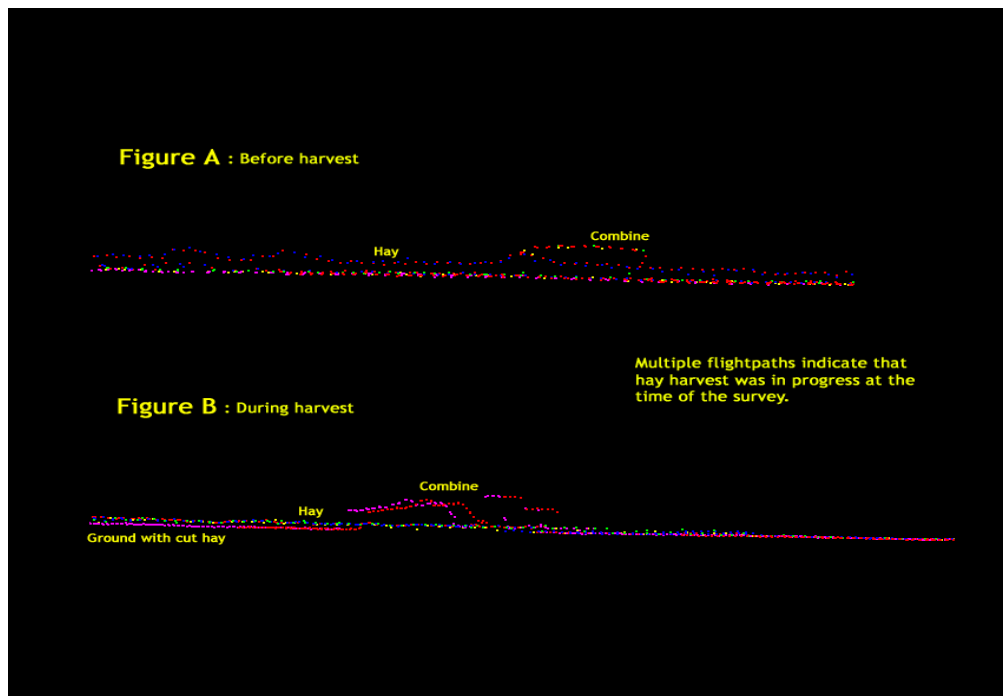


Figure 4. Example of short term land cover changes impact on vegetation model in agricultural fields.

3.4 Orthophotograph Processing

Image radiometric values were calibrated to specific gain and exposure settings associated with each capture using Leica's Calibration Post Processing software. The calibrated images were saved in tiff format to be used as inputs for the rectification process. Photo position and orientation was then calculated by assigning aircraft position and attitude information to each image by associating the time of image capture with trajectory file (SBET) in IPASCO. Photos were then orthorectified to the LiDAR derived ground surface using LPS. This typically results in <2 pixel relative accuracy discrepancy between images. Relative accuracy can vary slightly with terrain but offsets greater than 2 pixels tend to manifest at the image edges which are typically removed in the mosaic process.

The rectified images were mosaicked together in a three step process using Orthovista. First, color correction was applied to each image using global tilting adjustments designed to homogenize overlapping regions. Secondly, discrepancies between images were minimized by an automated seam generation process. The most nadir portion of each image was selected and seams were drawn around landscape features. The high resolution orthophotos were then delineated into a manageable size (~1500 x 1500 m) appropriate to the pixel resolution and requested spatial reference.

4. LiDAR Accuracy Assessment

4.1 Laser Noise and Relative Accuracy

Laser point absolute accuracy is largely a function of laser noise and relative accuracy. To minimize these contributions to absolute error, we first performed a number of noise filtering and calibration procedures prior to evaluating absolute accuracy.

Laser Noise

For any given target, laser noise is the breadth of the data cloud per laser return (i.e., last, first, etc.). Lower intensity surfaces (roads, rooftops, still/calm water) experience higher laser noise. The laser noise range for this survey was approximately 0.02 meters.

Relative Accuracy

Relative accuracy refers to the internal consistency of the data set - the ability to place a laser point in the same location over multiple flight lines, GPS conditions, and aircraft attitudes. Affected by system attitude offsets, scale, and GPS/IMU drift, internal consistency is measured as the divergence between points from different flight lines within an overlapping area. Divergence is most apparent when flight lines are opposing. When the LiDAR system is well calibrated, the line-to-line divergence is low (<10 cm). See Appendix A for further information on sources of error and operational measures that can be taken to improve relative accuracy.

Relative Accuracy Calibration Methodology

1. **Manual System Calibration:** Calibration procedures for each mission require solving geometric relationships that relate measured swath-to-swath deviations to misalignments of system attitude parameters. Corrected scale, pitch, roll and heading offsets were calculated and applied to resolve misalignments. The raw divergence between lines was computed after the manual calibration was completed and reported for each survey area.
2. **Automated Attitude Calibration:** All data were tested and calibrated using TerraMatch automated sampling routines. Ground points were classified for each individual flight line and used for line-to-line testing. System misalignment offsets (pitch, roll and heading) and scale were solved for each individual mission and applied to respective mission datasets. The data from each mission were then blended when imported together to form the entire area of interest.
3. **Automated Z Calibration:** Ground points per line were used to calculate the vertical divergence between lines caused by vertical GPS drift. Automated Z calibration was the final step employed for relative accuracy calibration.

4.2 Absolute Accuracy

Laser point absolute accuracy is largely a function of laser noise and relative accuracy. To minimize these contributions to absolute error, a number of noise filtering and calibration procedures were performed prior to evaluating absolute accuracy. The LiDAR quality assurance process uses the data from the real-time kinematic (RTK) ground survey conducted in the AOI. For this project a total of 546 RTK GPS measurements were collected on hard surfaces distributed among multiple flight swaths. To assess absolute accuracy the location coordinates of these known RTK ground points were compared to those calculated for the closest ground-classified laser points.

The vertical accuracy of the LiDAR data is described as the mean and standard deviation (sigma - σ) of divergence of LiDAR point coordinates from RTK ground survey point coordinates. To provide a sense of the model predictive power of the dataset, the root mean square error (RMSE) for vertical accuracy is also provided. These statistics assume the error distributions for x, y, and z are normally distributed, thus we also consider the skew and kurtosis of distributions when evaluating error statistics.

Statements of statistical accuracy apply to fixed terrestrial surfaces only and may not be applied to areas of dense vegetation or steep terrain (See Appendix A).

5. Photo Accuracy Assessment

True-color imagery was ortho rectified to the LiDAR data using direct georeferencing. The photo acquisition was conducted during the same flight as the 2010 LiDAR acquisition using the same positioning instrumentation. To assess spatial accuracy, the orthophotographs are compared against check points identified from the LiDAR intensity images. The check points were collected and measured on surface features identifiable in both images. The accuracy of the final mosaic, expressed as root mean square error (RMSE), was calculated in relation to the LiDAR-derived check points (Table 4). Figure 5 shows the co-registration between orthorectified photographs and LiDAR intensity images.

Figure 5. Example of co-registration of color images with LiDAR intensity images.



6. Study Area Results

Summary statistics for point resolution and accuracy (relative and absolute) of the LiDAR data collected in the Lemhi River, ID survey area are presented below in terms of central tendency, variation around the mean, and the spatial distribution of the data (for point resolution by tile).

6.1 Data Summary

Table 2. LiDAR Resolution and Accuracy - Specifications and Achieved Values.

	Targeted	Achieved
Resolution:	≥ 8 points/m ²	14.18 points/m ²
*Vertical Accuracy (1 σ):	<15 cm	2.5 cm

6.2 Data Density/Resolution

The average first-return density of delivered dataset is 14.18 points per square meter (Table 2). The initial dataset, acquired to be ≥ 8 points per square meter, was filtered as described previously to remove spurious or inaccurate points. Additionally, some types of surfaces (i.e., dense vegetation, breaks in terrain, water, steep slopes) may return fewer pulses (delivered density) than the laser originally emitted (native density).

Ground classifications were derived from automated ground surface modeling and manual, supervised classifications where it was determined that the automated model had failed. Ground return densities will be lower in areas of dense vegetation, water, or buildings.

As mentioned previously, portions of the 2009 acquisition have been combined with overlapping portions of the 2010 LiDAR acquisition to ensure a seamless transition. Consequently, some bins have a point density much greater than the targeted 8 points per square meter. Figures 8 and 9 show the distribution of average native and ground point densities for each processing bin.

Cumulative LiDAR data resolution for the Lemhi River, ID AOI:

- Average Point (First Return) Density = 14.18 points/m²
- Average Ground Point Density = 4.24 points/m²

Figure 6. Density distribution for first return laser points.

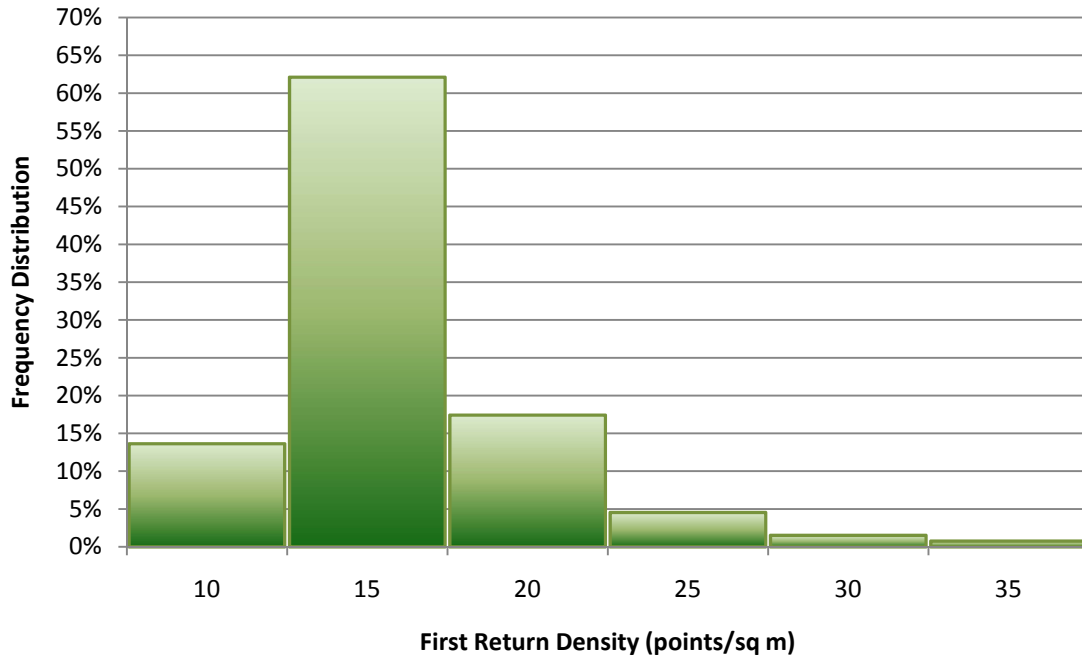


Figure 7. Density distribution for ground classified laser points.

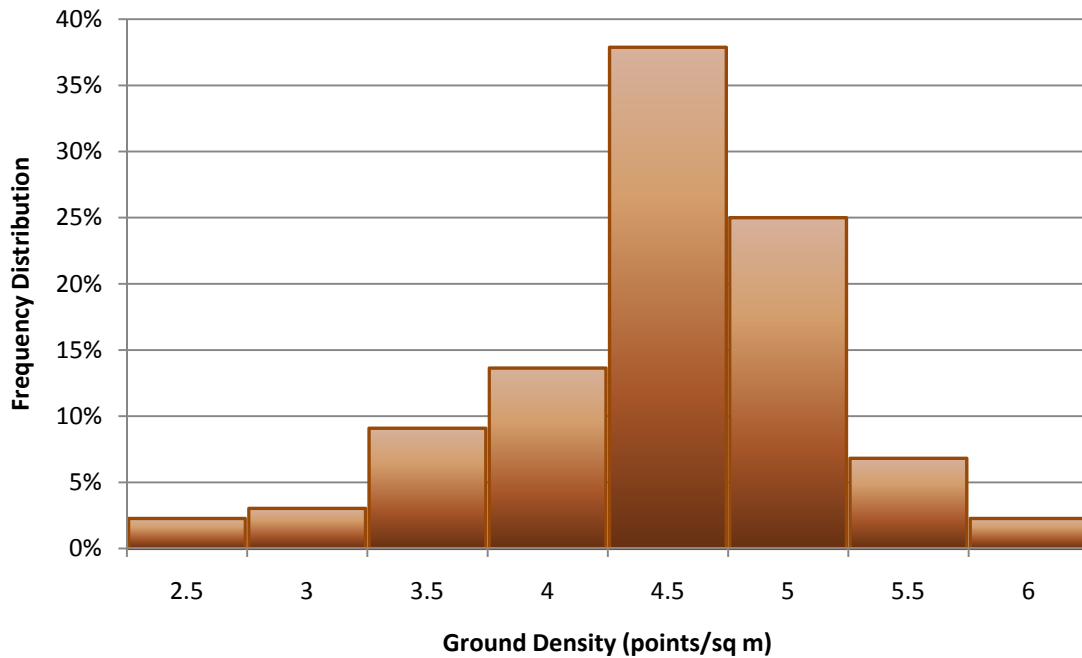


Figure 8. Density distribution map for first return points by processing bin.

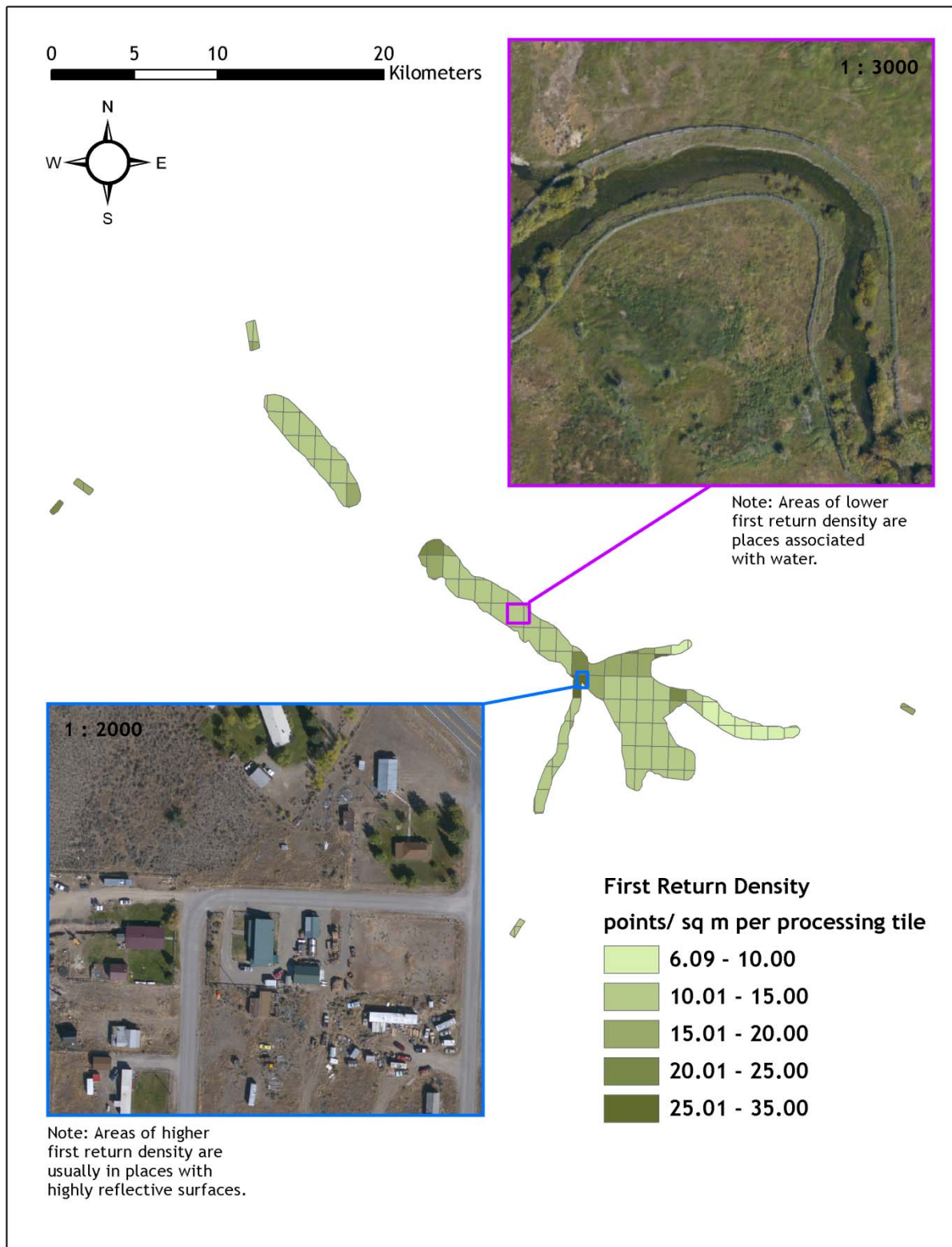
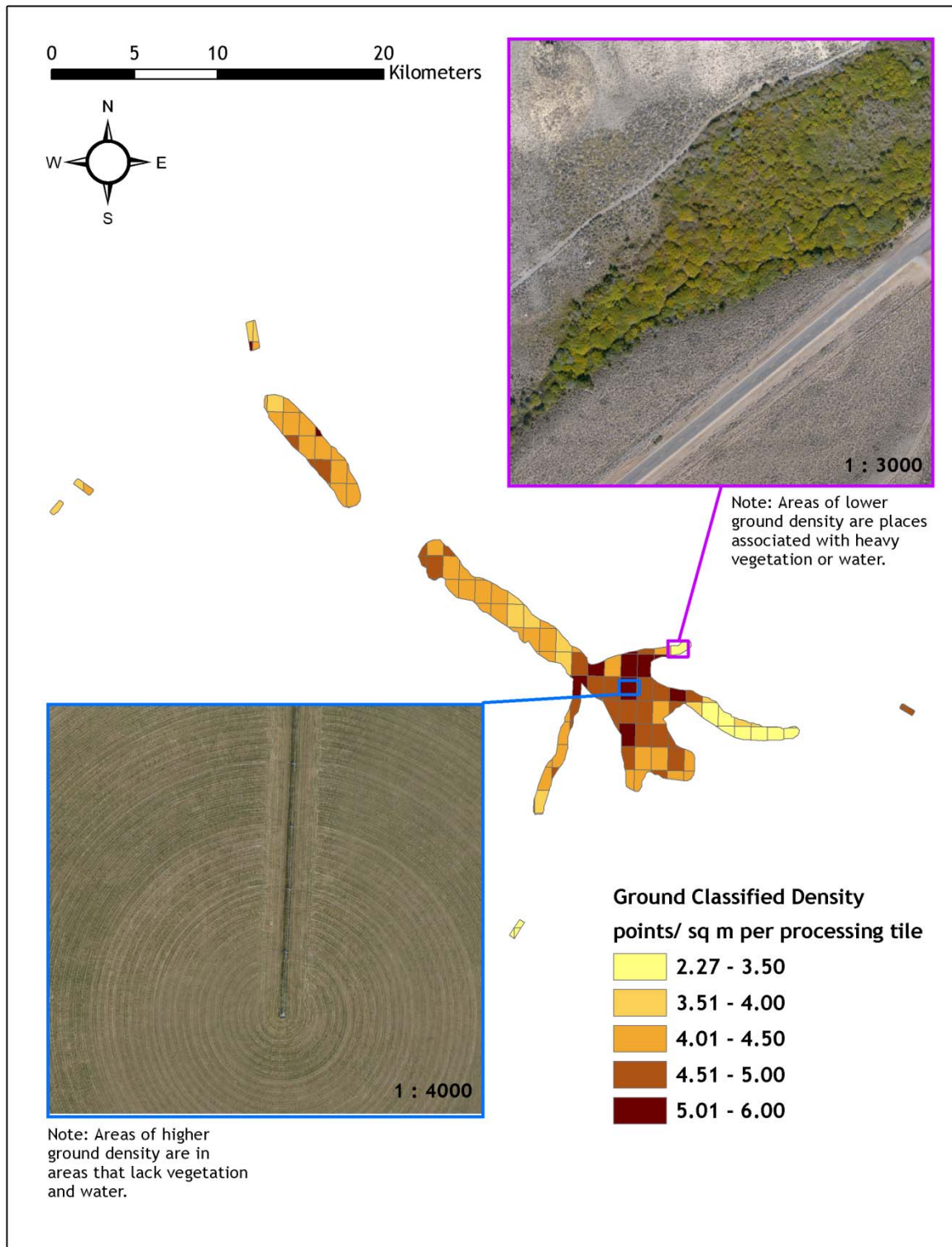


Figure 9. Density distribution map for ground return points by processing bin.

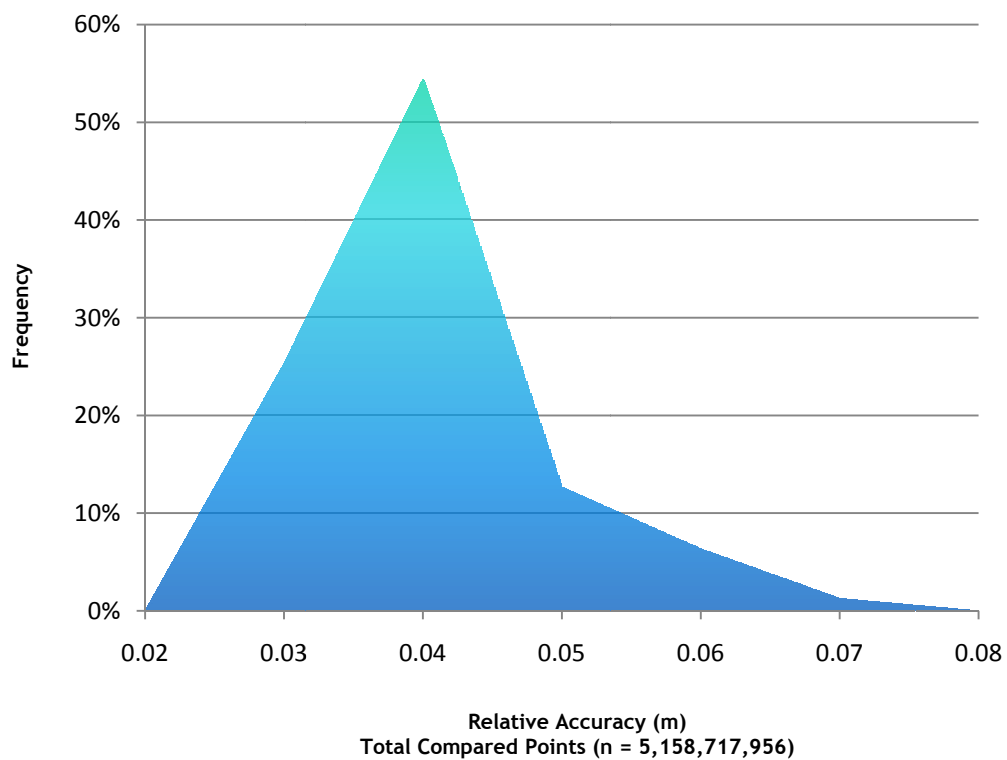


6.3 Relative Accuracy Calibration Results

Relative accuracy statistics for the Lemhi River, ID dataset measure the full survey calibration including areas outside the delivered boundary:

- Project Average = 0.032m
- Median Relative Accuracy = 0.033m
- 1σ Relative Accuracy = 0.011m
- 1.96σ Relative Accuracy = 0.021m

Figure 10. Distribution of relative accuracies per flight line, non slope-adjusted.



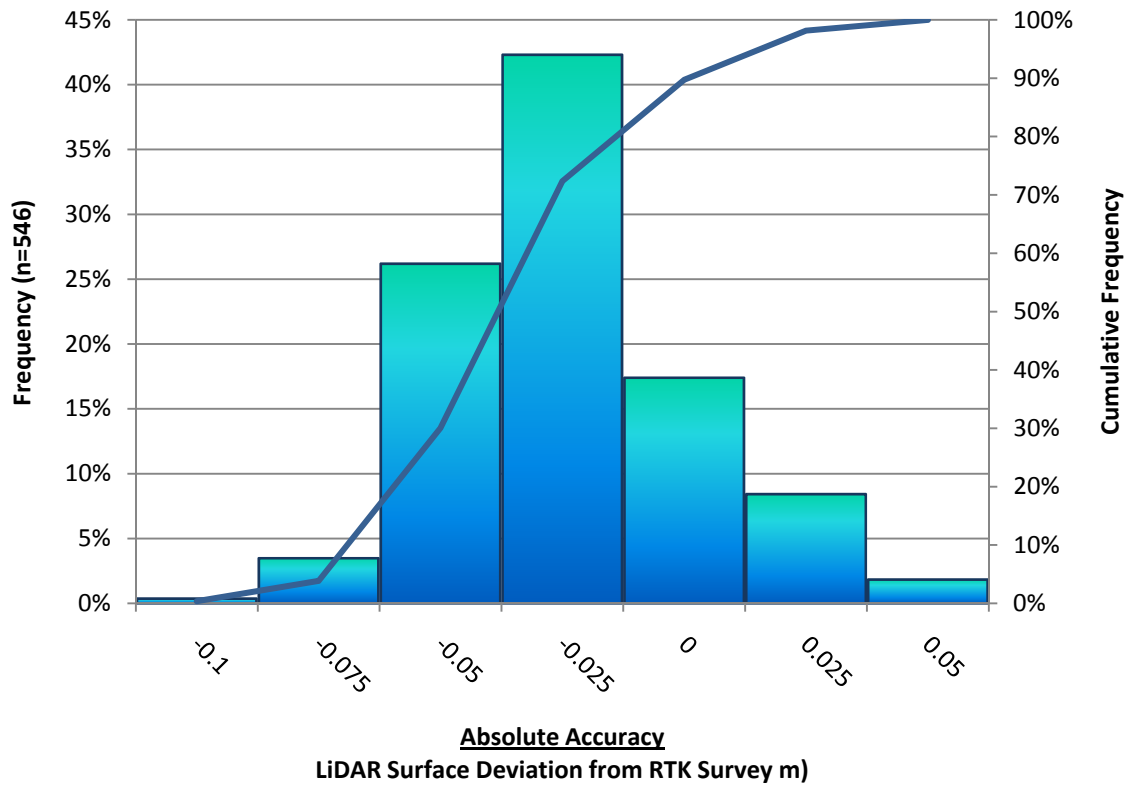
6.4 Absolute Accuracy

Absolute accuracies for the Lemhi River survey area:

Table 3. Absolute Accuracy - Deviation between laser points and RTK hard surface survey points.

RTK Survey Sample Size (n): 546		
Root Mean Square Error (RMSE) = 0.043m		Minimum Δz = -0.104m
Standard Deviations		Maximum Δz = 0.039m
1 sigma (σ): 0.025m	1.96 sigma (σ): 0.049m	Average Δz = -0.035m

Figure 11. Absolute Accuracy - Histogram Statistics.



6.5 Orthophotograph Accuracy

Figure 12. Orthophotograph check point location map for the Lemhi River study area.

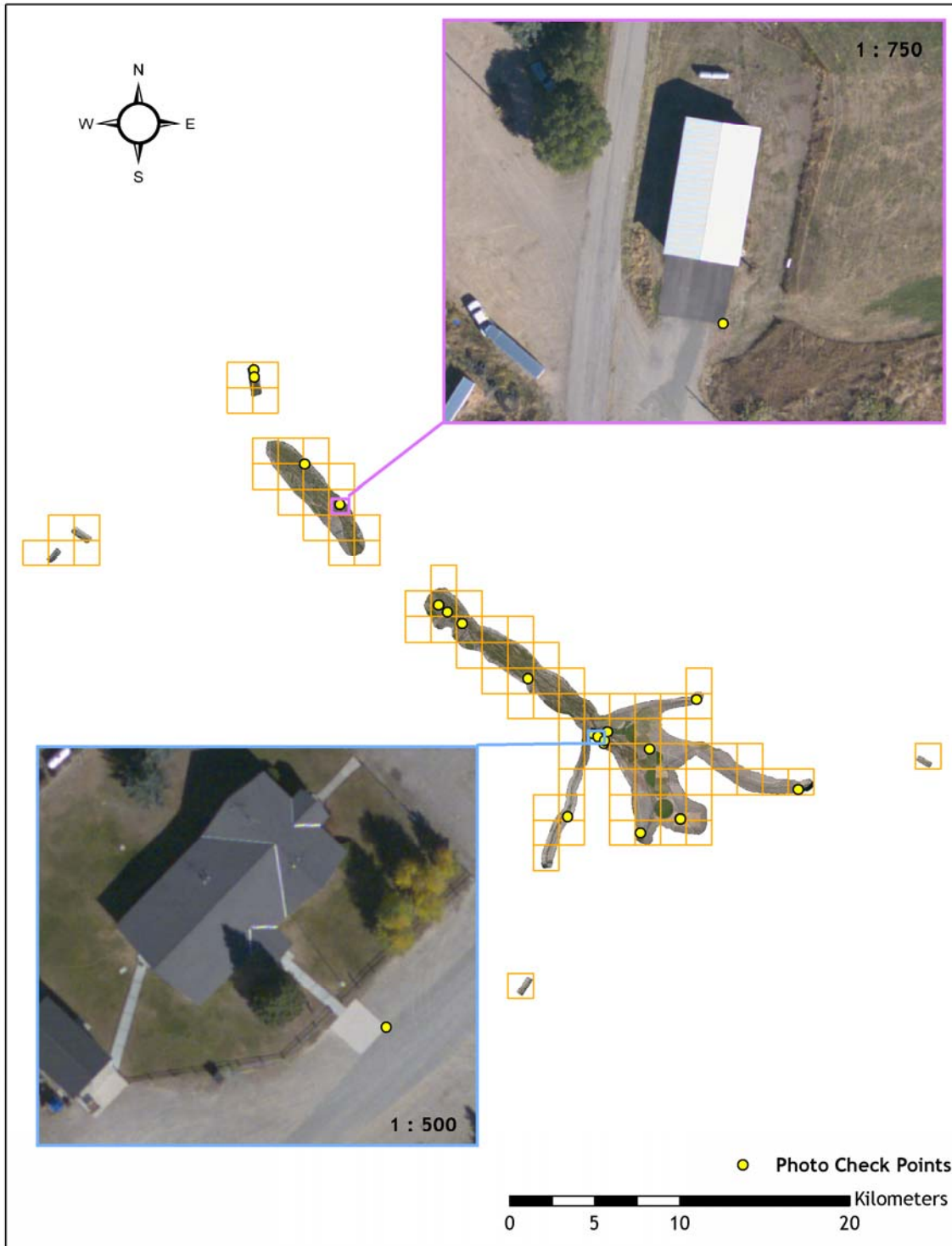
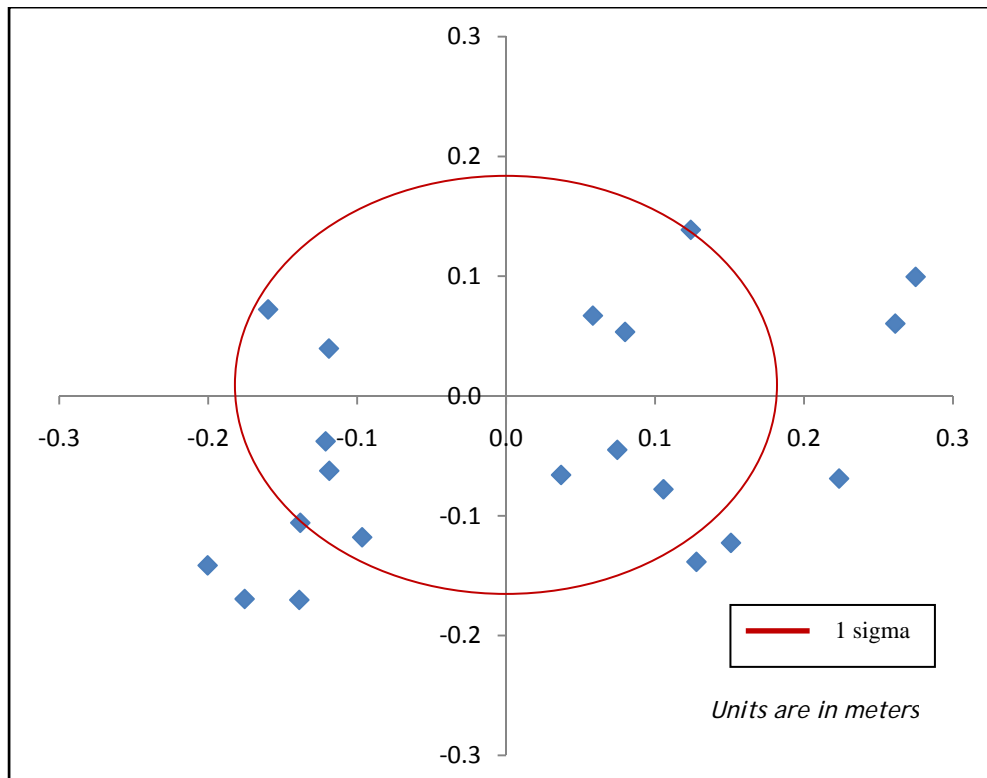


Table 4. Deviation between aerial photos and intensity images based on 20 accuracy check points.

	Mean	Standard Deviation (1 Sigma)	Root Mean Square Error (RMSE)
Lemhi River Photos	0.04 m	0.18 m	0.50 m

Figure 13. Checkpoint residuals derived from comparing aerial photos to intensity images.



7. Model Development

7.1 Breakline Enforced Terrain Model

David C. Smith and Associates (DSA) created breaklines for the Lemhi River study area using LiDAR-grammetry. **Table 5** describes the type and definition of each breakline collected. The breaklines were used to supplement the LiDAR data in creation of a hydro-enforced ground model.

- Water boundaries were enforced using hard breaklines and water surfaces were flattened based on the elevation from the breaklines. The breakline boundaries were also used to assign any points with ground or model key point classification within the water delineated areas as a water class.
- Hard breaklines (culverts, water islands, etc.) were incorporated into the TIN by enforcing triangle edges (adjacent to the breakline) to the elevation values derived from the LiDAR-grammetric breakline (Figure 14). This implementation corrected interpolation along the hard edge.
- For soft breaklines (provided as feature in Table 5), the breaklines aided ground classification of LiDAR points along a particular feature as well as capturing areas of occlusion in the LiDAR point cloud (e.g. a large tree masking a floodplain terrace).
- Culverts and artificial impediments to drainage flow were identified with hard breaklines. LiDAR data points within three meters of a culvert breakline were ignored from the ground classification, giving precedence to breakline Z values. This enforces proper drainage flow in development of the ground model.
- Stream centerlines were inspected in the ground model. ArcHydro Tools 9 was run on resulting ground models as a quality inspection of stream definition. (Figure 15) In areas where stream definition deviated from bare earth ground model and breaklines, LiDAR data was reexamined to provide increased detail (adding or subtracting appropriate ground classified points).

Table 5. Breaklines collected for the Lemhi River study area.

Feature	Implementation	Description
Breakline	Hard Breakline	breaklines to supplement the lidar
Culvert	Hard Breakline	high confidence culvert crossing
Culvert Connect	Hard Breakline	low confidence culvert crossing
Water Stream	Hard Breakline	double line streams (large)
Water Island	Hard Breakline	islands
Water Lake	Hard Breakline	lake bodies
Water Stream Single	Provided as Feature	single line streams (small)
Ditch Bottom	Provided as Feature	man made ditches
Drain Bottom	Provided as Feature	drainage
Road Centerline	Provided as Feature	road centerlines
Levee Centerline	Provided as Feature	top of levee, centerline

Figure 14. Example of situation where, because of dense vegetation, an in-stream island ground surface was not captured with the laser but was identified with LiDARgrammetric breaklines.

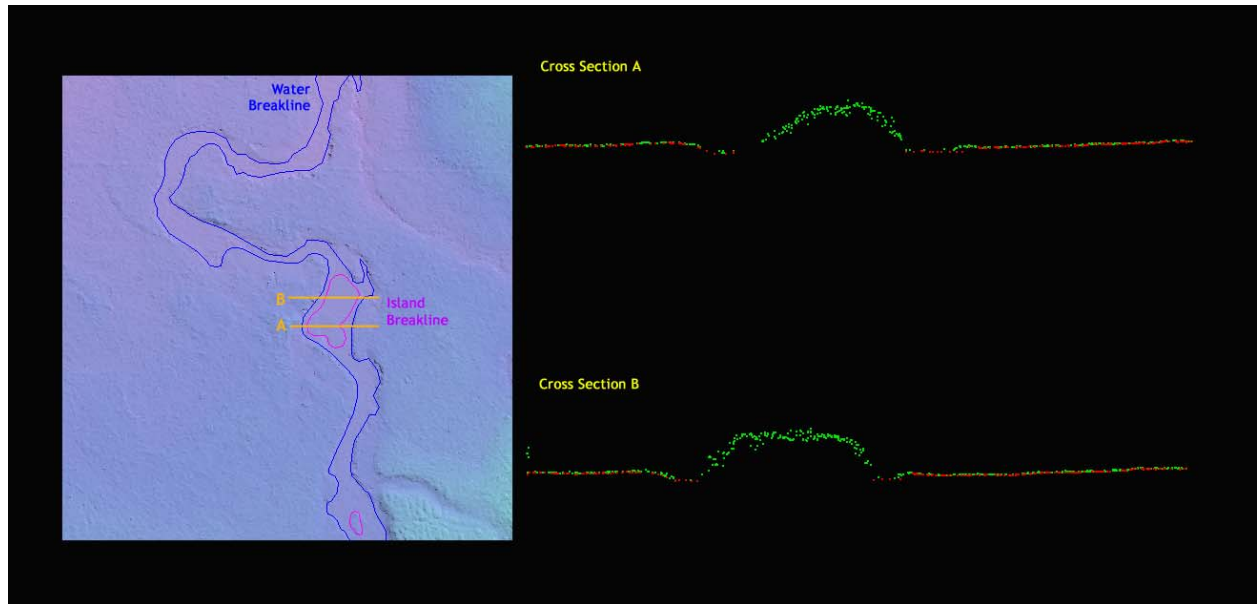


Figure 15. ArchHydro Tools 9 Stream Direction laid over LiDAR bare earth hillshade.

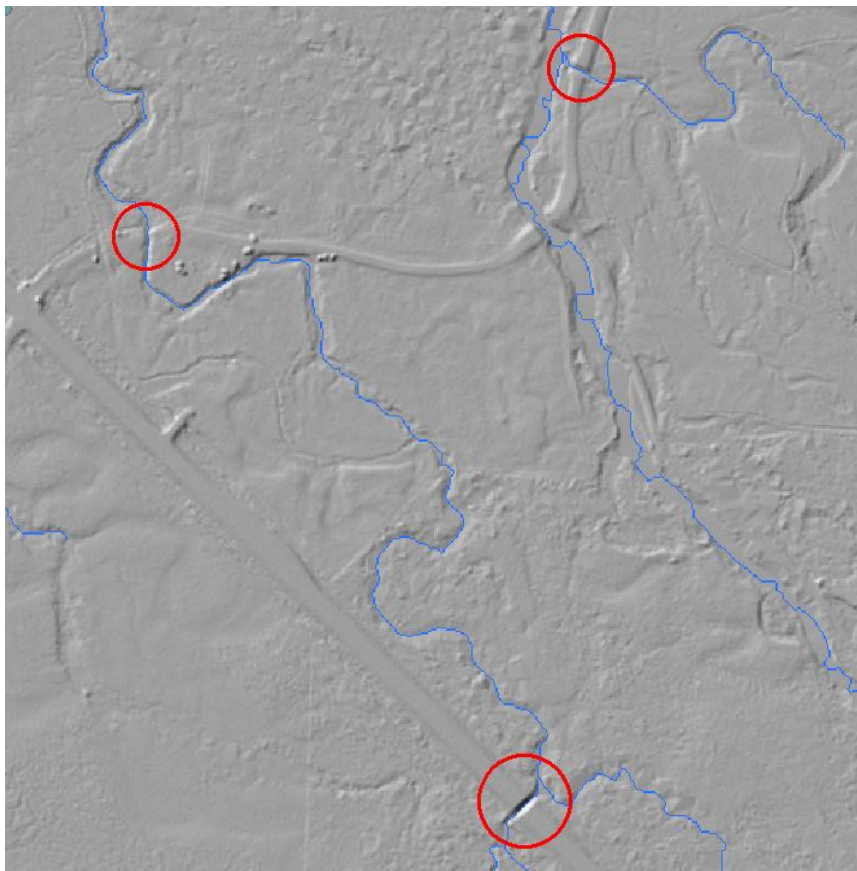
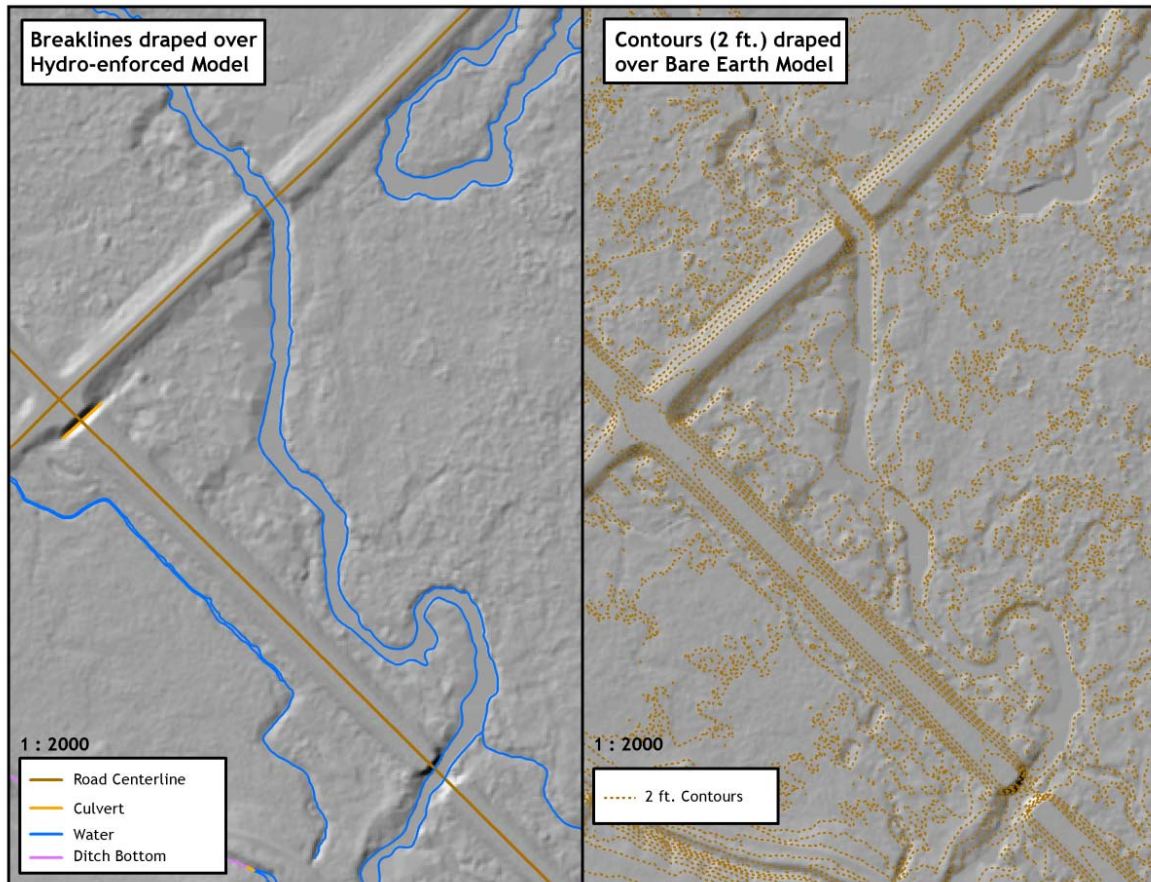


Figure 16. Comparison between hydro-enforced (left) and non hydro-enforced (right) bare earth models.



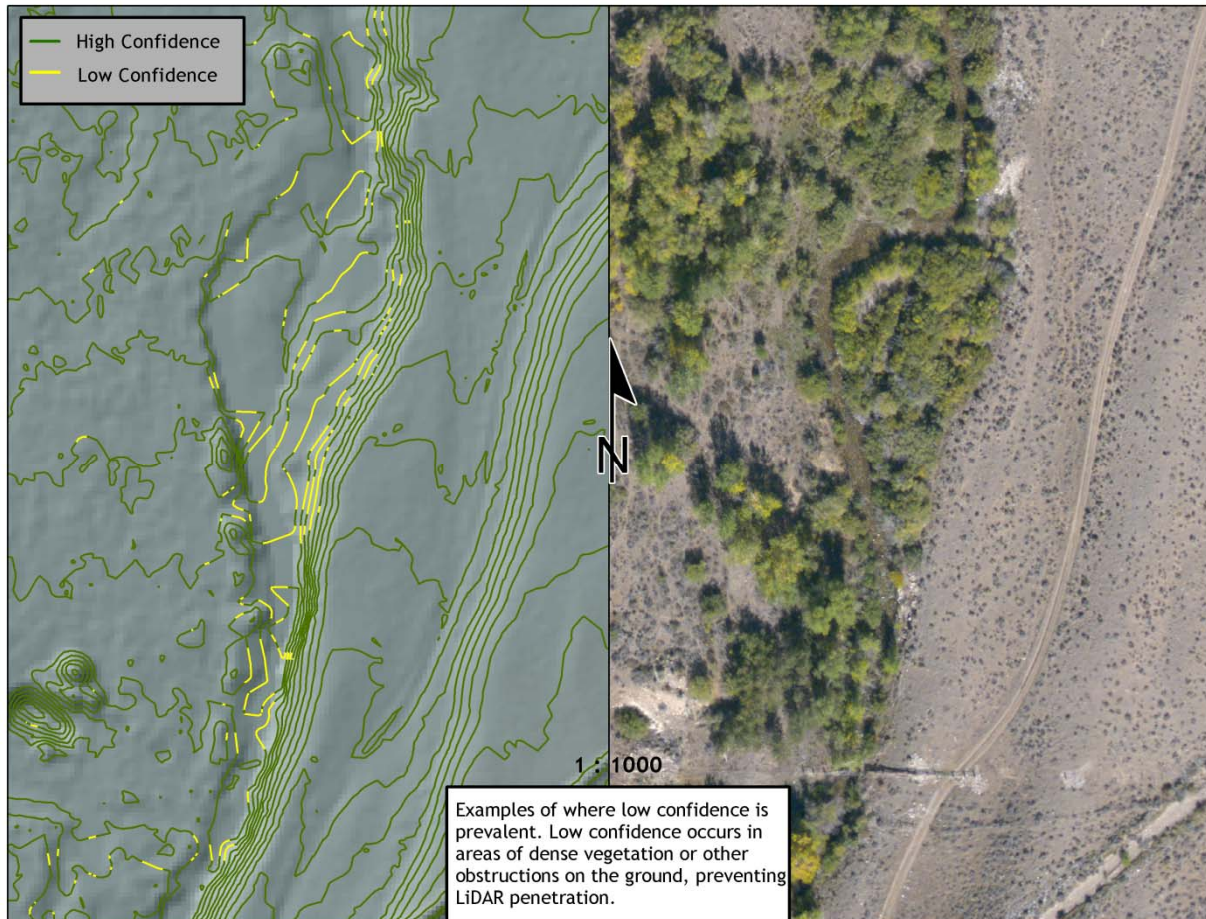
7.2 Vegetation Surface Model

The vegetation surface model (VSM) was generated by outputting a gridded surface using returns classified as vegetation (section 3.3.1). In areas void of vegetation, the bare earth model was used as the default surface. The result is a 1-m elevation model combining the vegetation canopy surface and bare-earth (where vegetation was not present). As discussed earlier, all points that were ≤ 25 cm above the ground surface were excluded from the vegetation classified points and therefore from the resulting vegetation surface model.

8. Contours

Contour key points were classed out of the ground model every 20 feet to provide a more manageable dataset to work with (provided no significant change in Z). Contours were produced through TerraModeler with a Z tolerance of .25 feet. Contours were output in .dxf file format and have been converted to an ESRI feature class. The same breakline rules and resulting ground class for the hydro-flattened ground model were used as the basis for contour creation.

Figure 17. Examples of low and high contour confidence.



9. Projection/Datum and Units

	Projection:	UTM Zone 12, NAD 83
Datum	Vertical:	NAVD88 Geoid03
	Horizontal:	NAD83
	Units:	meters

10. Deliverables

Point Data:	<p>LAS 1.2 format</p> <ul style="list-style-type: none"> • All Returns • Ground points • Vegetation points <p>ASCII format</p> <ul style="list-style-type: none"> • All Returns • Ground points • Vegetation points
Vector Data:	<ul style="list-style-type: none"> • Tile Index of LiDAR Points (shapefile format) • Orthophoto Tile Delineation (shapefile format) • Digital Surface Models Index (shapefile format) • Study area boundary (shapefile format)
Raster Data:	<ul style="list-style-type: none"> • Elevation Models (1 m resolution) <ul style="list-style-type: none"> • Bare Earth Model (ESRI GRID format) • Hydro-flattened/Enforced (ESRI GRID format) • Vegetation Surface (ESRI GRID format) • Intensity Images (GeoTIFF format, 0.5 m resolution) • Orthophoto Tiles (GeoTIFF format 15 cm resolution)
Data Report:	<ul style="list-style-type: none"> • Full report containing introduction, methodology, and accuracy



11. Selected Images

Figure 18. Imagery draped over 3D point cloud looking southwest at Hawley Creek.

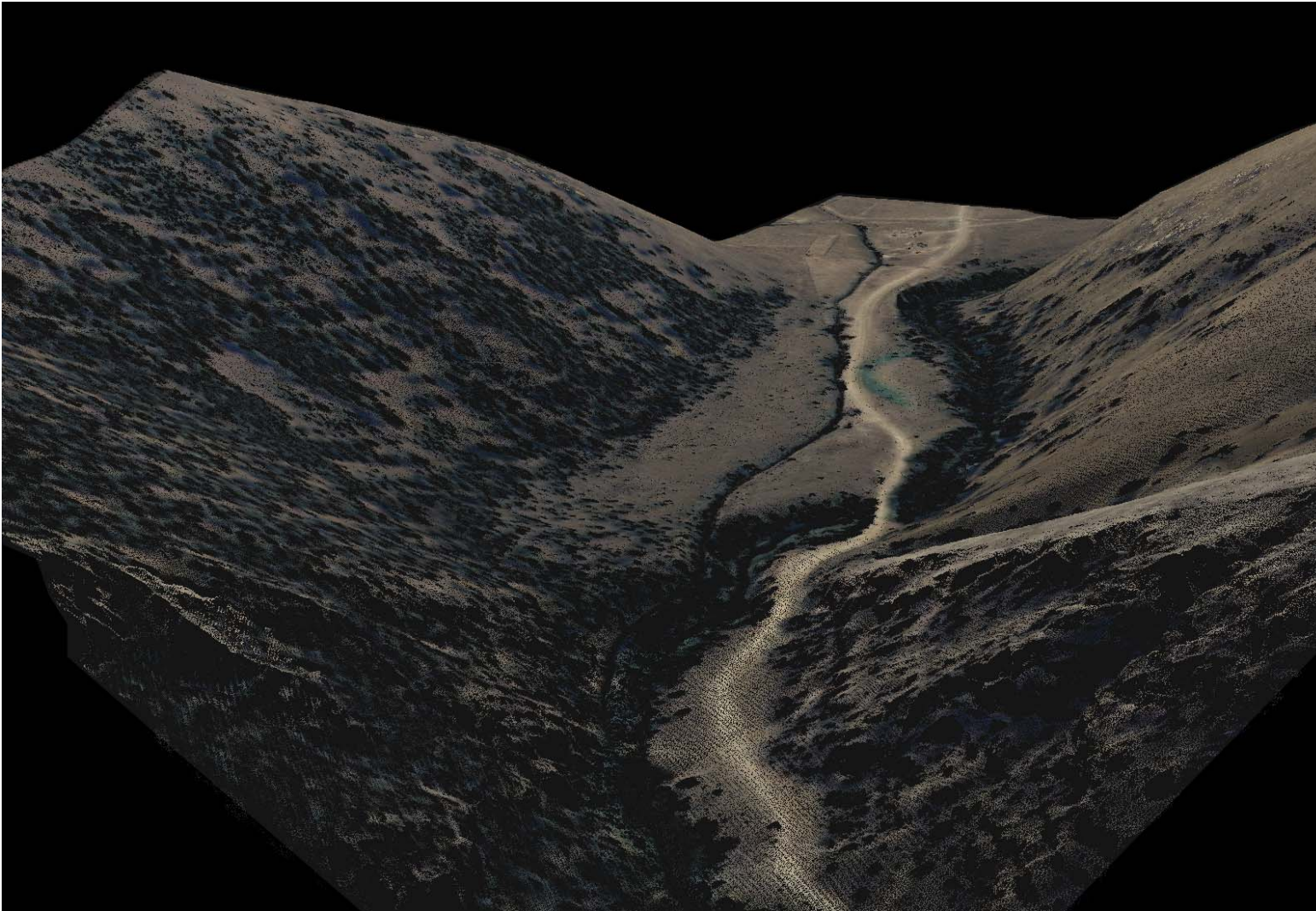
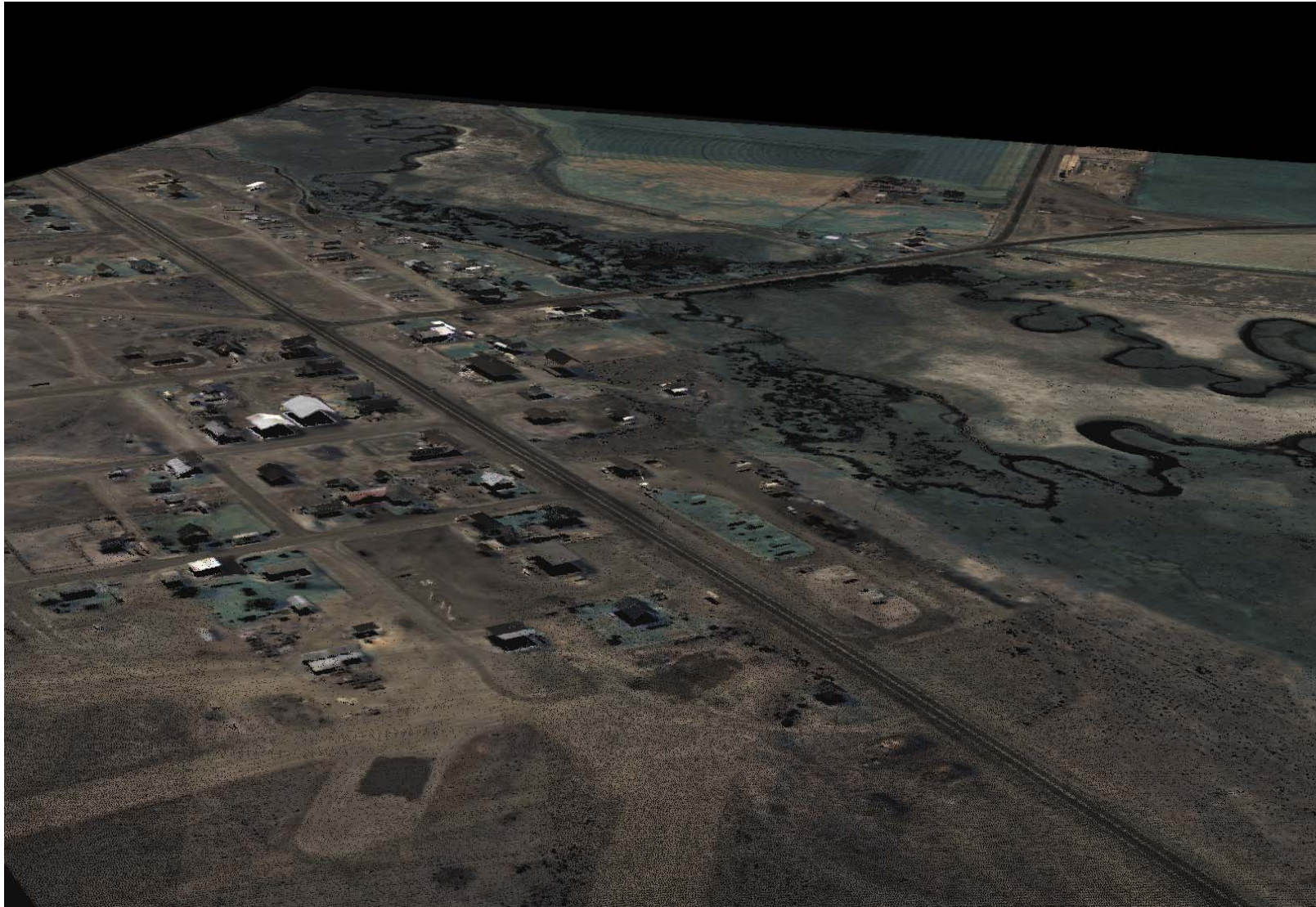


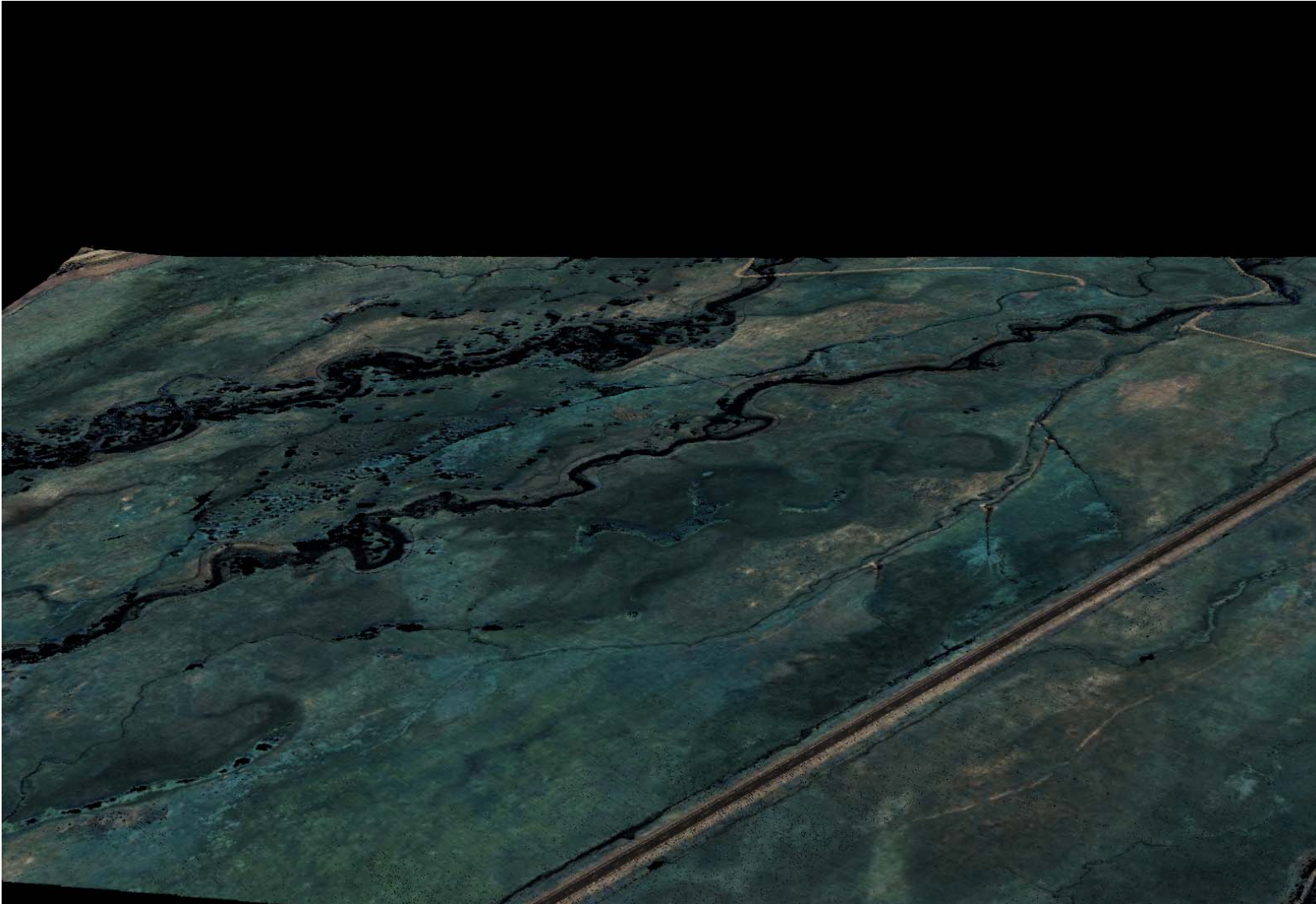
Figure 19. Imagery draped over 3D LiDAR point cloud looking northeast at the city of Leadore.



LiDAR Data Acquisition and Processing: Lemhi River, ID

Prepared by Watershed Sciences, Inc.

Figure 20. Imagery draped over a 3D LiDAR point cloud looking northeast at the Lemhi River floodplain with State Highway 28 in the foreground.



LiDAR Data Acquisition and Processing: Lemhi River, ID

Prepared by Watershed Sciences, Inc.

Figure 21. Imagery draped over a 3D LiDAR point cloud, looking southwest at a plateau with State Highway 28 running through the center.

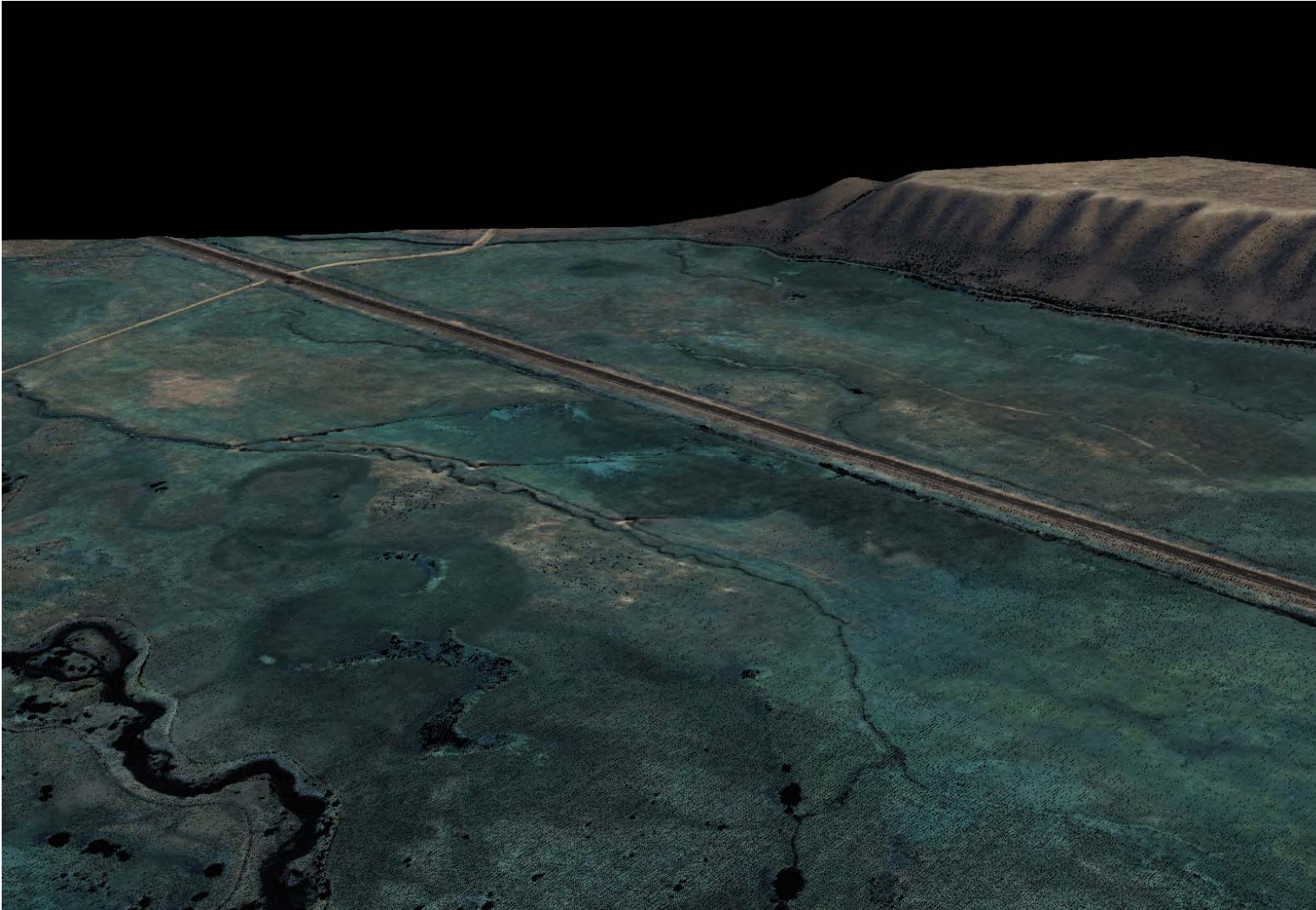


Figure 22. 3D LiDAR point cloud looking at a rocky outcrop near the southern end of the study area.

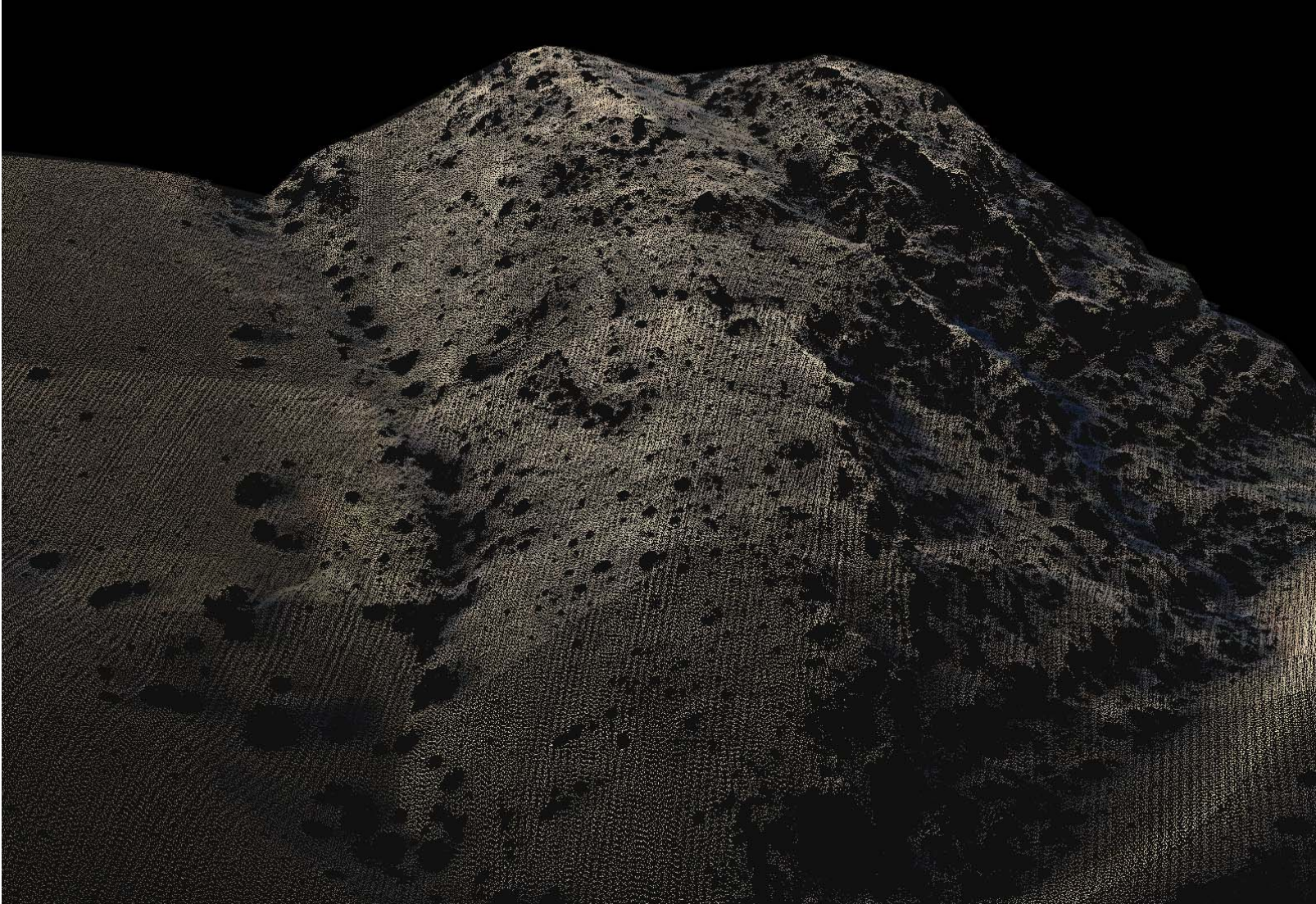


Figure 23. Bare earth model colored by elevation, looking across the Lemhi River floodplain at Old Highway 28.

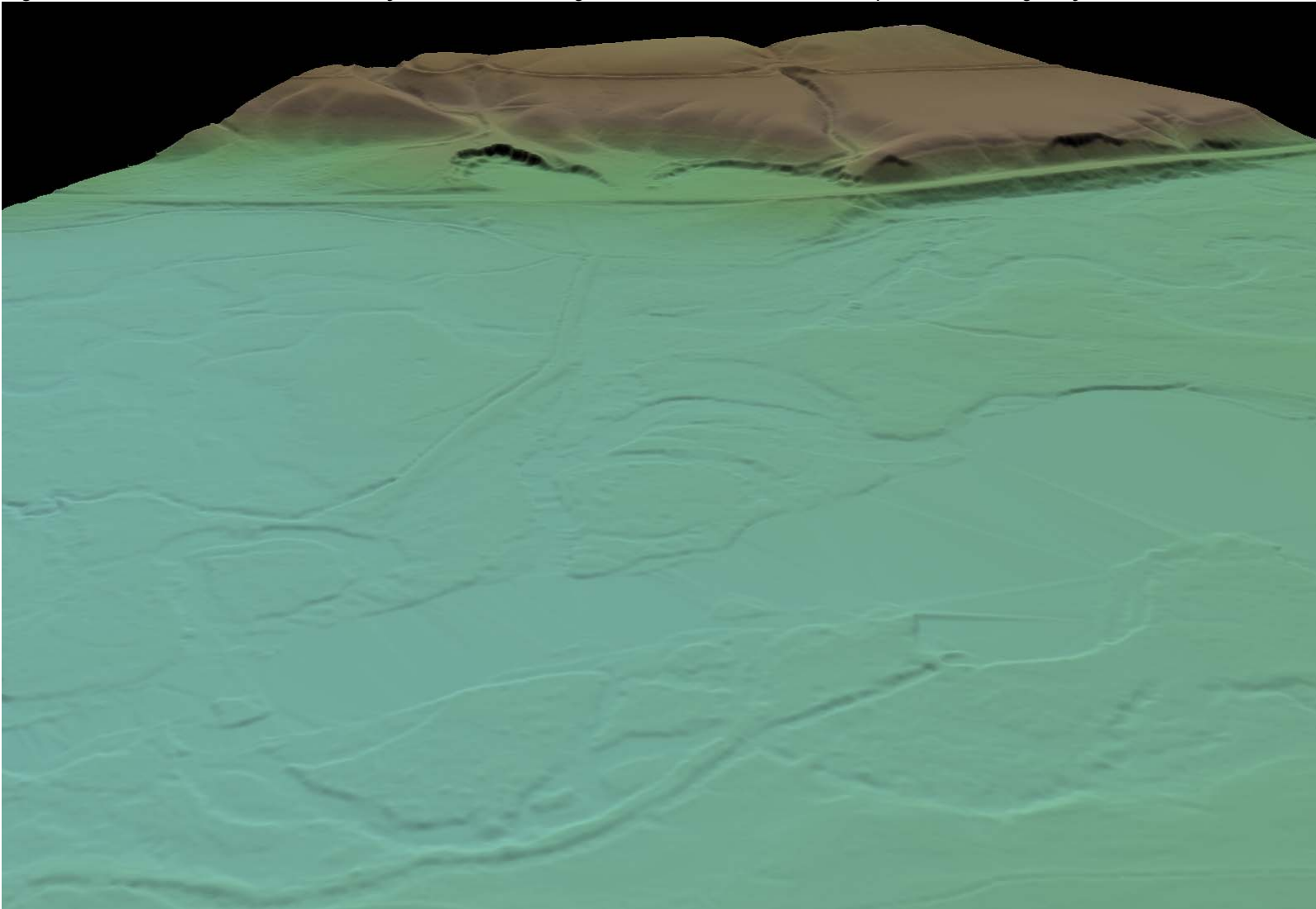


Figure 24. Bare earth model colored by elevation, looking east at the Lemhi River stream morphology.

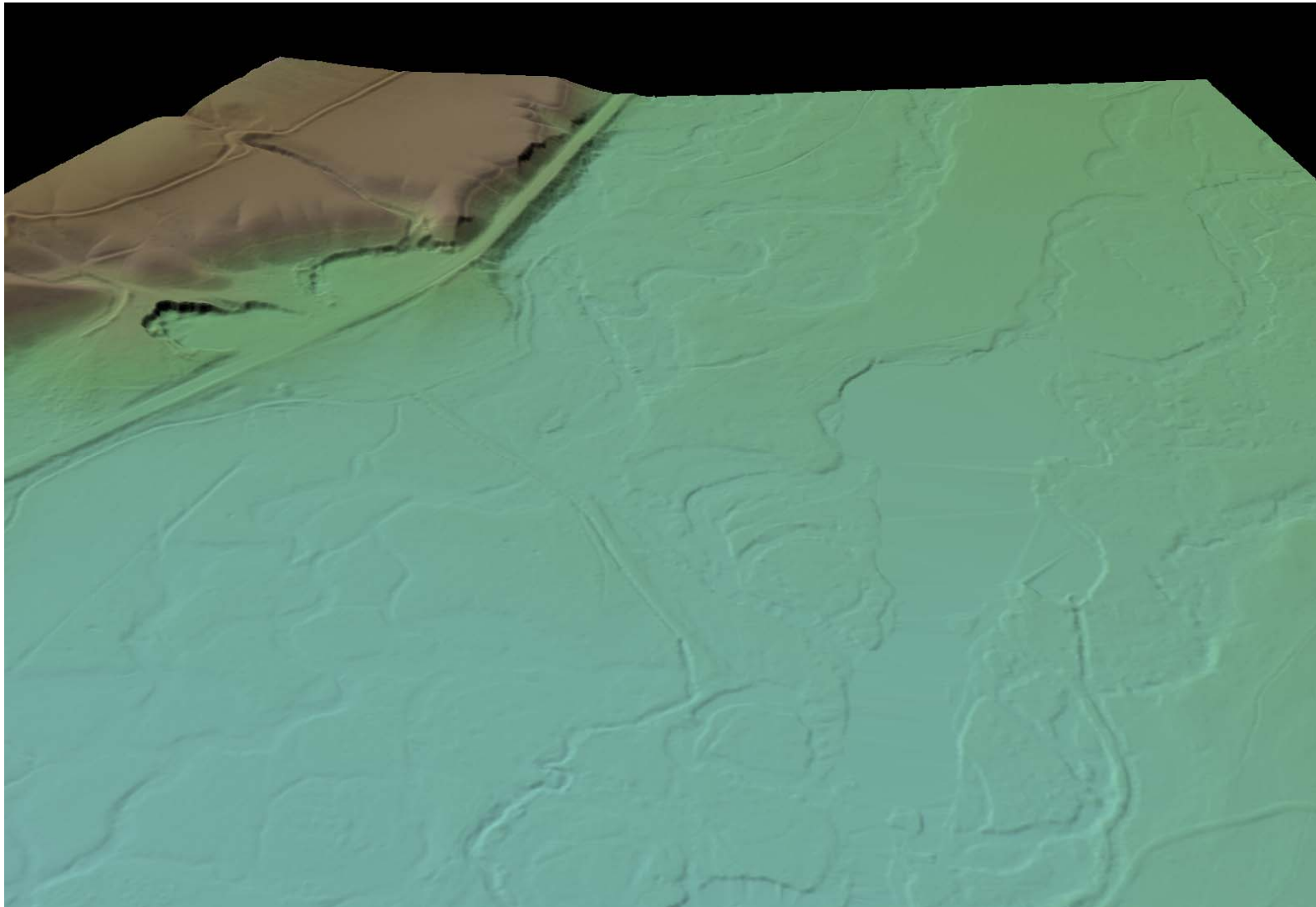
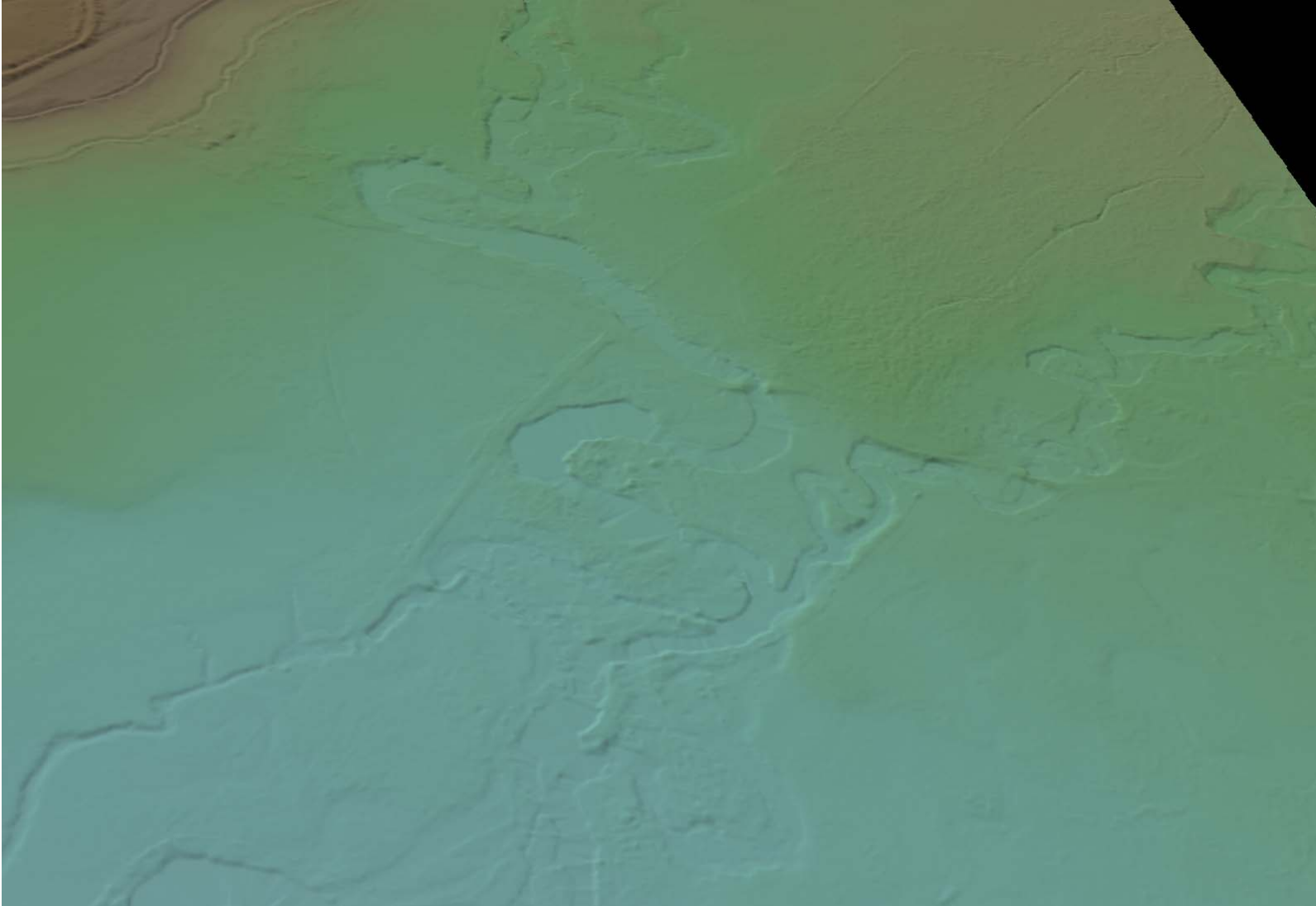


Figure 25. Bare earth model colored by elevation, looking south east at the Lemhi River.



12. Glossary

1-sigma (σ) Absolute Deviation: Value for which the data are within one standard deviation (approximately 68th percentile) of a normally distributed data set.

1.96-sigma (σ) Absolute Deviation: Value for which the data are within two standard deviations (approximately 95th percentile) of a normally distributed data set.

Root Mean Square Error (RMSE): A statistic used to approximate the difference between real-world points and the LiDAR points. It is calculated by squaring all the values, then taking the average of the squares and taking the square root of the average.

Pulse Rate (PR): The rate at which laser pulses are emitted from the sensor; typically measured as thousands of pulses per second (kHz).

Pulse Returns: For every laser pulse emitted, the Leica ALS 50 Phase II system can record *up to four* wave forms reflected back to the sensor. Portions of the wave form that return earliest are the highest element in multi-tiered surfaces such as vegetation. Portions of the wave form that return last are the lowest element in multi-tiered surfaces.

Accuracy: The statistical comparison between known (surveyed) points and laser points. Typically measured as the standard deviation (σ) and root mean square error (RMSE).

Intensity Values: The peak power ratio of the laser return to the emitted laser. It is a function of surface reflectivity.

Data Density: A common measure of LiDAR resolution, measured as points per square meter.

Spot Spacing: Also a measure of LiDAR resolution, measured as the average distance between laser points.

Nadir: A single point or locus of points on the surface of the earth directly below a sensor as it progresses along its flight line.

Scan Angle: The angle from nadir to the edge of the scan, measured in degrees. Laser point accuracy typically decreases as scan angles increase.

Overlap: The area shared between flight lines, typically measured in percents; 100% overlap is essential to ensure complete coverage and reduce laser shadows.

DTM / DEM: These often-interchanged terms refer to models made from laser points. The digital elevation model (DEM) refers to all surfaces, including bare ground and vegetation, while the digital terrain model (DTM) refers only to those points classified as ground.

Real-Time Kinematic (RTK) Survey: GPS surveying is conducted with a GPS base station deployed over a known monument with a radio connection to a GPS rover. Both the base station and rover receive differential GPS data and the baseline correction is solved between the two. This type of ground survey is accurate to 1.5 cm or less.

13. Citations

Soininen, A. 2004. TerraScan User's Guide. TerraSolid.

Appendix A

LiDAR accuracy error sources and solutions:

Type of Error	Source	Post Processing Solution
GPS (Static/Kinematic)	Long Base Lines	None
	Poor Satellite Constellation	None
	Poor Antenna Visibility	Reduce Visibility Mask
Relative Accuracy	Poor System Calibration	Recalibrate IMU and sensor offsets/settings
	Inaccurate System	None
Laser Noise	Poor Laser Timing	None
	Poor Laser Reception	None
	Poor Laser Power	None
	Irregular Laser Shape	None

Operational measures taken to improve relative accuracy:

1. Low Flight Altitude: Terrain following is employed to maintain a constant above ground level (AGL). Laser horizontal errors are a function of flight altitude above ground (i.e., ~ 1/3000th AGL flight altitude).
2. Focus Laser Power at narrow beam footprint: A laser return must be received by the system above a power threshold to accurately record a measurement. The strength of the laser return is a function of laser emission power, laser footprint, flight altitude and the reflectivity of the target. While surface reflectivity cannot be controlled, laser power can be increased and low flight altitudes can be maintained.
3. Reduced Scan Angle: Edge-of-scan data can become inaccurate. The scan angle was reduced to a maximum of $\pm 15^\circ$ from nadir, creating a narrow swath width and greatly reducing laser shadows from trees and buildings.
4. Quality GPS: Flights took place during optimal GPS conditions (e.g., 6 or more satellites and PDOP [Position Dilution of Precision] less than 3.0). Before each flight, the PDOP was determined for the survey day. During all flight times, a dual frequency DGPS base station recording at 1-second epochs was utilized and a maximum baseline length between the aircraft and the control points was less than 19 km (11.5 miles) at all times.
5. Ground Survey: Ground survey point accuracy (i.e. <1.5 cm RMSE) occurs during optimal PDOP ranges and targets a minimal baseline distance of 4 miles between GPS rover and base. Robust statistics are, in part, a function of sample size (n) and distribution. Ground survey RTK points are distributed to the extent possible throughout multiple flight lines and across the survey area.
6. 50% Side-Lap (100% Overlap): Overlapping areas are optimized for relative accuracy testing. Laser shadowing is minimized to help increase target acquisition from multiple scan angles. Ideally, with a 50% side-lap, the most nadir portion of one flight line coincides with the edge (least nadir) portion of overlapping flight lines. A minimum of 50% side-lap with terrain-followed acquisition prevents data gaps.
7. Opposing Flight Lines: All overlapping flight lines are opposing. Pitch, roll and heading errors are amplified by a factor of two relative to the adjacent flight line(s), making misalignments easier to detect and resolve.